12-2004

Cure Behavior Study and Elastic Modulus Characterization of Resin System of a Quasi Poloidal Stellarator Modular Coil

Hariharanath Kavuri
University of Tennessee - Knoxville

To the Graduate Council:

I am submitting herewith a thesis written by Hariharanath Kavuri entitled "Cure Behavior Study and Elastic Modulus Characterization of Resin System of a Quasi Poloidal Stellarator Modular Coil." I have examined the final electronic copy of this thesis for form and content and recommend that it be accepted in partial fulfillment of the requirements for the degree of Master of Science, with a major in Mechanical Engineering.

Madhu S. Madhukar, Major Professor

We have read this thesis and recommend its acceptance:

Masood Parang, Kevin M. Kit

Accepted for the Council:
Carolyn R. Hodges

Vice Provost and Dean of the Graduate School

(Original signatures are on file with official student records.)

To the Graduate Council:

I am submitting herewith a thesis written by Hariharanath Kavuri entitled "Cure Behavior Study and Elastic Modulus Characterization of Resin System of a Quasi Poloidal Stellarator Modular Coil". I have examined the final electronic copy of this thesis for form and content and recommend that it be accepted in partial fulfillment of the requirements for the degree of Master of Science, with a major in Mechanical Engineering.

Madhu S. Madhukar
Major Professor

We have read this thesis and
recommend its acceptance:

Masood Parang

Kevin M. Kit

Acceptance for the Council:

Anne Mayhew

Vice Chancellor and Dean of
Graduate studies

(Original signatures are on the file with official student records.)

CURE BEHAVIOR STUDY AND ELASTIC MODULUS CHARACTERIZATION OF RESIN SYSTEM OF A QUASI POLOIDAL STELLERATOR MODULAR COIL

A Thesis Presented for the
Master of Science
Degree
The University of Tennessee, Knoxville

Hariharanath Kavuri

December 2004

DEDICATION

This thesis is dedicated to my parents, Rama Prasad and Varalakshmi, my sister, Bhargavi, and my brother, Kalyan.

ACKNOWLEDGMENTS

I would like to express my gratitude to Dr. Madhu S. Madhukar for his great support, guidance and belief in me. He has been a great advisor and mentor to me and I have gained immensely from his knowledge and experience. This work is a result of his encouragement and timely ideas. I thank my committee members, Dr. Masood Parang and Dr. Kevin M. Kit, for their valuable suggestions and encouragement provided to me.
I thank Dr. Brad Nelson, Fusion Energy Division, Oak Ridge National Labs, for his support and guidance. I would like to thank Oak Ridge National labs for their financial support throughout the length of my study.

I would like to thank Mr. Dennis Higdon of the electronics shop for all the technical support he provided. I would like to thank my lab mate, Richard Burgess, who spared his time for all the discussions we had about this research.

I am greatly indebted to my parents, Sri. Rama Prasad and Smt. Varalakshmi, my sister Bhargavi, my brother Kalyan, for their unrelenting support, love and encouragement. I would like to thank my seniors Teja Sastry Kuruganti, Krishna Kanth Inavolu, Kiran Sagi and my friends Anuj, Rohan, Sampath, and Mohan for their helpful suggestions and support. Lastly, I would like to thank all my college friends and other family members for all their support and encouragement.

ABSTRACT

Composites materials are increasingly becoming choice materials because of their tremendous strength-to-weight properties and impressive design flexibility. A more recent application of composites is in nuclear fusion reactors. One such reactor is the Quasi-Poloidal Stellarator (QPS) being developed by Oak Ridge National laboratory. QPS, with a non-axisymmetric, near-poloidally symmetric magnetic configuration, has stranded copper/epoxy composite coils, used for magnetic confinement of plasma. CTD-404 and CTD-101K are the resins under consideration for the modular coils with copper fiber as reinforcement. Structural integrity of the modular coils over wide range of temperatures, including liquid nitrogen temperature, is of vital importance and appropriate resin with optimal cure cycle has to be used for this purpose.

In this regard, a study of the stresses induced on the fibers during cure of CTD-404 and CTD-101K was performed using the Cure Induced Stress Test (CIST) setup at UT composites laboratory. Carbon fiber was used for comparison purposes. It was observed that both CTD-404 and CTD-101K induced low cure stresses and high cool down stresses.

Later in this study a new method was developed to calculate the elastic modulus of a resin during cure. The knowledge of elastic modulus development of a resin during cure is vital in minimizing the residual stresses by appropriately changing the parameters of cure cycle. The method was developed based on difference in the displacements of the

resin sample during cure, with fiber and without fiber. The method was developed for 3501-6 as the volume change data for CTD-101K and CTD-404 were not available. The volume change data for 3501-6, obtained by using volumetric dilatometer previously, was used and the load data of the reinforced fiber was obtained from cure-induced stress test. The curve for elastic modulus was developed for two isothermal cure cycles. Results obtained were compared with available experimental data and the data available in literature from three-point bend tests of cured samples at different cure times. The values of modulus obtained with this approach compared well with the available data.

Also, a study of the effect of liquid nitrogen temperature on the elastic modulus of the modular coil composite was performed. A fixture was designed to perform a cantilever bend test in liquid nitrogen on a MTS machine. It was observed that the liquid nitrogen temperature did not affect the modulus.

TABLE OF CONTENTS

LIST OF TABLES

LIST OF FIGURES

1. BACKGROUND

Modern structural composites, frequently referred to as advanced composites, are blends of two or more materials, one of which is composed of stiff, long fibers and, for polymeric composites, a resinous binder or matrix that holds the fibers in place. Modern composite materials evolved from the simplest mixtures of two or more materials to obtain a property that was not there before. Composites have many advantages when compared to conventional materials which include high strength to weight ratio, longer life and inherent damping. Composites are widely applied in a range of fields viz. aerospace, automotive, sporting goods to marine applications [1].

A more recent application of composites is in nuclear fusion reactors. Quasi-poloidal stellarator, being developed by Oak Ridge National labs, has stranded copper/epoxy composite coils, used for magnetic confinement of plasma, made of composite materials.

1.1 QUASI-POLOIDAL STELLARATOR:

The critical need for Non-fossil fuel energy sources is increasing and energy from nuclear fusion is the best choice owing to the availability of abundant fuel and low-radioactive emission from reactions.

Stellarators are the second approach, after Tokamaks, in generating energy from fusion. Stellarators are a class of magnetic fusion confinement devices characterized by three

dimensional magnetic fields and plasma shapes and are the best-developed class of magnetic fusion devices after the tokomaks. The Quasi-Poloidal Stellarator (QPS), currently in the early design phase, is a low-aspect ratio, concept exploration experiment with a non-axisymmetric, near-poloidally symmetric magnetic configuration.

1.2 STELLARATOR CORE - COMPOSITES:

The Stellarator core consists of the *modular coil set* that provides the primary magnetic field configuration, *auxiliary coils* including vertical field coils, toroidal field coils, and an ohmic current solenoid, machine structure, and an external vacuum vessel. A cut-away view of the Stellarator is provided in Figure 1.1.

The modular coils, in particular, have to be conformed to specific shapes so as to produce a magnetic field that will contain the plasma. The geometry of the coils has been generated using physics optimization codes, such that the cross-section of the coil is capable of carrying the required current.

All coils are of conventional construction, wound from hollow copper conductor and insulated with glass-epoxy. Other winding options such as a “dry cable”: design with no epoxy impregnation, have been considered but these would require significant R&D to provide confidence that conductor motion would not cause fatigue failure. It is very unlikely that a winding using all-solid conductor would be feasible due to highly contoured winding path.

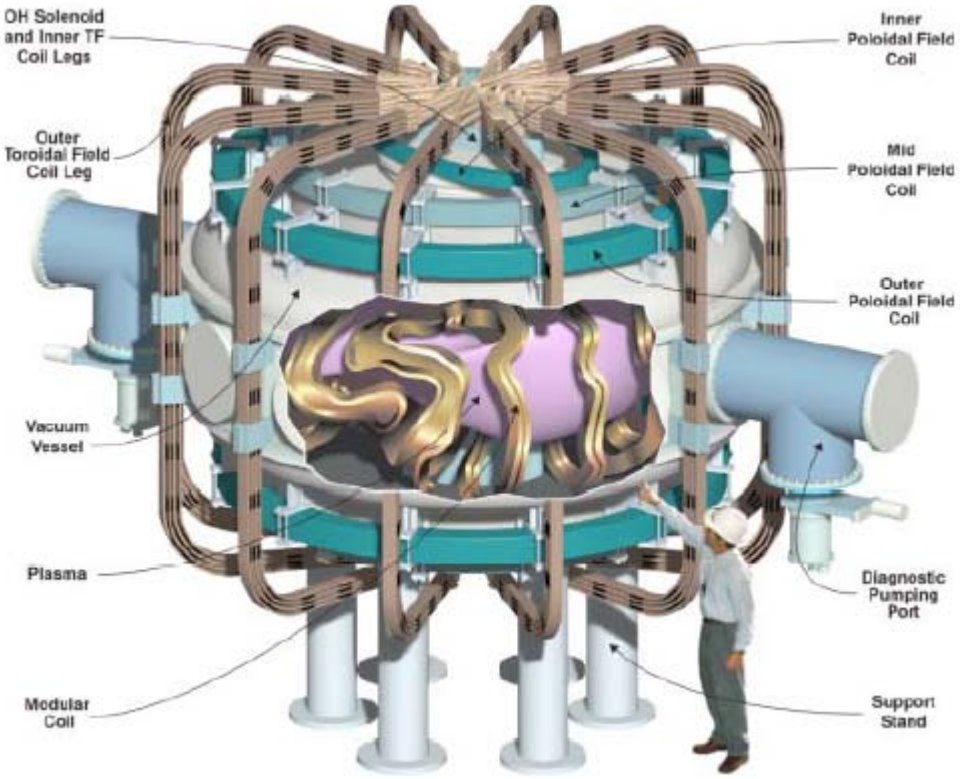

Figure 1.1: A cut-away view of the QPS

1.3 COILS CONSTRUCTION:

The preferred option for the coil conductor is a flexible cable design. The primary advantage of the flexible cable design is low cost, both to purchase the conductor and to wind it A typical design would consist of a standard braided cable of fine copper wire (36 gage, for example) that would be pulled through a "turks head" into a rectangular cross section (figure 1.2).

The conductor would be wrapped with fiberglass tape and hand wound into the winding cavity of the coil form (figure 1.3). One disadvantage is that the conductor has little inherent strength, and must be almost continuously supported by the integral coil structure. For modular coils, the windings are wound on and supported by the tee-shaped structural member, which is an integral part of the coil winding form (figure 1.4).

Once a single layer of conductor is in place a series of chill plates are installed and the second layer of conductor is wound into place. The chill plates consist of a copper sandwich containing a serpentine cooling passage with inlet and outlet pipes for the gas cooling. The chill plates avoid the need for cooling the conductor internally, which is impractical for the turn lengths needed for QPS. Gas cooling is used to avoid electrical failure modes common to water cooled coils. After winding is complete, the final geometry is verified and the assembly is vacuum pressure impregnated with epoxy to complete the insulation system.

Auxiliary coils including vertical field coils, toroidal field coils, and an ohmic current solenoid are constructed in the same way.

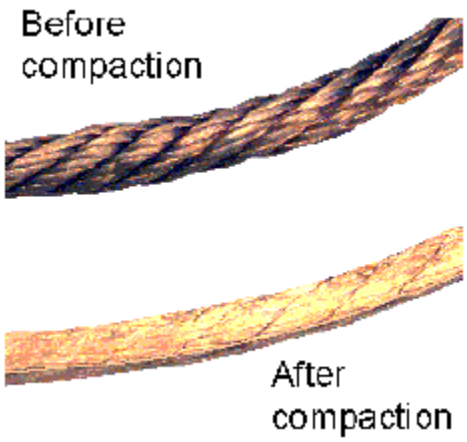

Figure 1.2: Copper cable before and after compaction

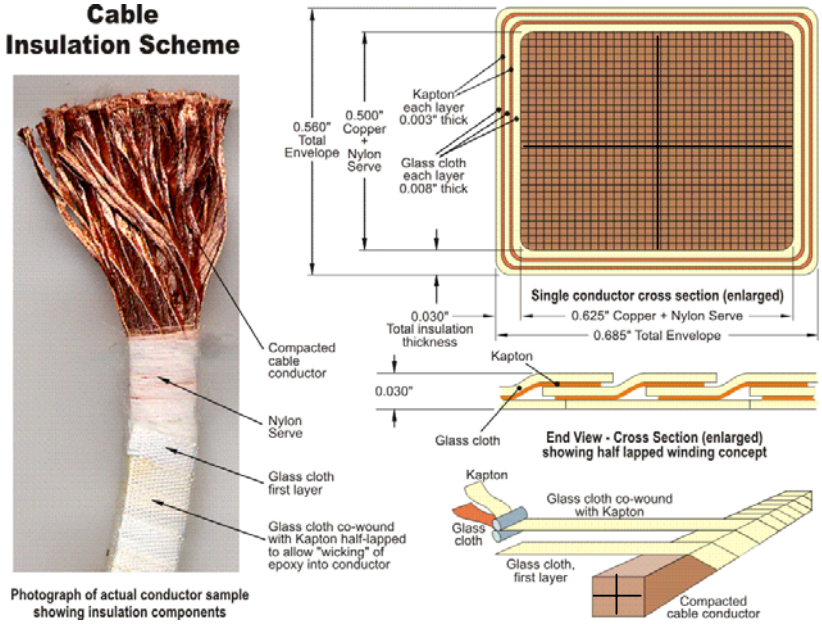

Figure 1.3: Glass-Kapton insulation of copper-epoxy composite

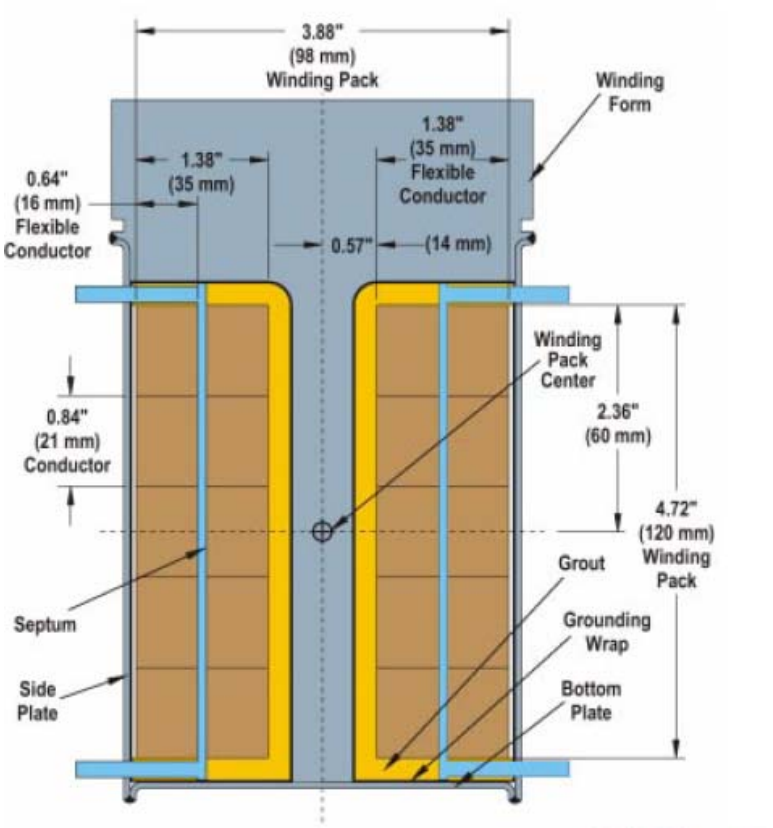

Figure 1.4: Modular coil winding cross-section

1.4 QPS COIL ISSUES: SELECTION OF EPOXY FOR THE COILS:

The epoxy resins under consideration for the modular and auxiliary coils are CTD-101K and CTD-404. Both resins are from Composite Technology Development Inc. Based on the resin behavior during cure, ease of handling, scope of cure cycle change, appropriate epoxy resin has to be selected.

A better understanding of cure-induced stress development for each of the above resins is required for the selection. These stresses are induced by volumetric changes occurring

during the cure process as well as during cool down. The effect of residual stresses generated during curing is reflected in the mechanical properties of cured composites [4]. The residual stresses that develop on the micro and macro levels can cause micro cracks in the coils. In addition, these stresses result in geometrical distortion of the part, which is highly undesirable for QPS coils.

The knowledge of residual stresses is very useful in understanding the resin behavior and can be used to modify the cure cycle. Cure cycles can be modified to develop the desired final properties of the resin. Also the description of the evolution of mechanical properties is useful in modifying the cure cycle.

Another issue is the low temperature operation of QPS coils which has been discussed in the final chapter. The need for the cryogenic cooling of QPS coils and the experiment to determine the modulus of the CTD-404 –Copper composite was described.

1.5 COMPOSITE CURING- ISSUES:

Curing is a very important phase in the processing of composites. Curing is the process where the properties of a thermosetting resin are irreversibly changed by chemical reaction, i.e. condensation, ring closure or addition. The cure of the thermosetting resin may be accomplished by addition of curing agent/hardener, which causes the resin to polymerize. The cure can be done with or without application of pressure.

In the curing of composites, one of the common problems is the presence of residual stresses in the composites. A stress developed on the fiber during the curing and cool down of the resin is always an area of concern. Shrinkage occurs during cure and cool down of the thermoset. Shrinkage during cool down is the thermal shrinkage of the resin. Whenever there is shrinkage in the resin, stresses are developed on the fiber. These residual stresses are undesired as they lead to warpage, delamination, micro cracking and related problems. In the thermoset polymer composites, the residual stresses are attributed to its inhomogeneous structure.

Research work has been going on in the area of composites processing. In the next chapter, a literature review is presented giving an account of previous research in this area. Also scope of the present work is described.

2. LITERATURE REVIEW

Measuring residual stresses, degree of cure, characterizing the evolution of mechanical properties and optimizing and modifying the cure cycles, have been some of the major areas of research for achieving optimal processing conditions for fiber reinforced polymer composites. Theoretical and experimental studies have been used to understand stress build up during cure and cool down. Effects of cure cycle parameters on different physical properties of the resin have been studied.

Madhukar et.al [5-7] did extensive work to study the stresses on fibers and modify the cure cycles for better composite properties. Fomitchov et.al [8] developed a laser-ultrasonic system for real-time monitoring of the cure state of polymer matrix composite parts. The system was integrated with a Resin Transfer Molding (RTM) machine, and contained (i) a fiberized laser array ultrasonic source and (ii) an embedded ultrasonic sensor based on an intrinsic fiber optic Sagnac interferometer. Bulk ultrasonic waves generated by the laser source were transmitted into the composite structure and were subsequently detected by the embedded ultrasonic sensor. The cure state was inferred from measurements of ultrasonic velocity in the composite part. Degamber et.al [9] demonstrated a non-contact method to determine the cure of a resin-hardener system. They used a non contact fiber optic probe in a custom modified microwave oven to record the near-infrared (NIR) spectra of a thermoset during cure. Real time cure monitoring was achieved at 4 different power levels inside microwave oven.

Other more recent works are process cure monitoring of unsaturated polyester resins by Raman Spectroscopy [10], monitoring resin flow and cure with a high-frequency electromagnetic wave transmission line constructed inside a structure [11], Real-time prediction of cure cycle performance in polymer composite processing using neural networks [12].

DeMeuse et.al [13] characterized the cure behavior of a complex thermosetting isocyanate/epoxy reactive mixture using torsional braid analysis (TBA) technique and the continuous heating (CHT) and isothermal time–temperature–transformation (TTT) cure diagrams. Hong-Bing Wang et.al [14] showed that varying cure temperature produces change of cure behavior, resulting in different residual stresses. They also showed that on elevating the cure temperatures, the residual stresses increase while decreasing the apparent gelation time. It was observed that compared to the thermal shrinkage during cool down, the curing shrinkage stresses are much smaller.

Blest et.al [15] performed the modeling and simulation of resin flow, heat transfer and the curing of multilayer thermoset composite laminates during processing in an autoclave. Darcy's Law and Stokes' slow-flow equations were used for the flow model and, for approximately isothermal flows, a similarity solution was developed. This permitted the decoupling of the velocity and thermal fields. A two-dimensional convection–diffusion heat equation with an internal heat generation term was then solved numerically, together with the equation for the rate of cure, using a finite difference scheme on a moving grid.

Skordos et.al [16] developed a non-parametric procedure for modeling of the chemical cure kinetics of a commercial resin-transfer-molding epoxy resin, RTM6. The procedure is entirely numerical and involves interpolation between experimentally determined values of cure reaction rates without any information about the chemical nature of process.

Bailleul et.al [17] developed a methodology to control the curing of composite material based on an inverse method. The method would be a method of optimization in which one is searching for an optimal cycle from the cure model allowing to minimize a criterion chosen according to a specific objective. Qi Zhu et.al [18] developed a three-dimensional coupled thermo-chemo-viscoelastic model to simulate the heat transfer, curing, residual stresses and deformation of a composite part during the entire cure cycle. White et.al [19] developed a process model used to predict the residual stress history during the curing of composite laminates. The model included the effects of chemical and thermal strains and assumed the material to exhibit linear viscoelastic behavior. They validated the model in a later work [20].

Gopal et.al [21] achieved optimal cure cycles by optimally varying the process parameters. Numerical simulation of a process model with input controllable parameters helped to observe the trends and characteristics of residual stress history. The gradients of the applied temperatures at different dwell times were identified as essential process parameters and based on this observation an optimized cure cycle was developed using the results of the parametric study.

Elastic modulus data during cure gives us an insight as to how the degree of cure can be expressed in terms of modulus. This data can help in optimizing the cure process for attaining the desired properties of resin system. Creep testing in three-point bend was used for specimens past gelation, to find the cure dependent modulus [22]. Time-temperature and time-conversion superposition principles were built into a model that successfully predicts the visco-elastic properties of the epoxy after gelation [23]. Meredith [24] developed a technique to measure the change in the elastic modulus during polymerization of resin-based materials using resonance frequency analysis. The technique is not sensitive to temperature and does not influence the polymerization.

Jakob [25] investigated the solidification behavior of a dimethacrylate system during UV and thermal cure at temperatures from the glass transition temperature (Tg) of the monomer to above the ultimate Tg of the polymer using torsional dynamic mechanical analysis. The method of cure was found to influence the properties of the cured material. When prepared above the ultimate Tg of the polymer, the UV cured material had a higher Tg, a higher crosslink density, and a higher degree of conversion than the thermally cured material. YongSom Eom et.al [26] calculated the relaxation modulus of an epoxy-amine resin system. An autocatalytic reaction model was used in the early stage of curing reaction and an nth-order kinetic model coupled with a diffusion-controlled reaction was applied to the later stage of reaction.

Madhukar et.al developed a method to characterize stiffness from volume change data and fiber-load data [27]. The slope of load-strain curve was considered proportional to the instantaneous value of polymer stiffness. Using similar data with an alternate

approach, here we propose a methodology to characterize the modulus development during cure. The methodology uses the difference in linear displacements of the polymer, with fiber and without fiber, during cure.

2.1 SCOPE OF PRESENT WORK:

I. A study of the stress development on fiber during the cure and cool down of CTD-404 and CTD-101K polymers was completed. Fibers used were Copper and carbon. The carbon fiber was used for comparison purposes. The Cure Induced Stress Test (CIST) setup developed at UT Composite Materials lab was used to perform cure cycle on the resin. Standard cure cycles from CTD Inc. were used for the resins.

II. A new method was developed to estimate the Young's modulus of CTD-101 and CTD-404 polymer during cure from the volume change data and fiber – load data.

III. Experiments were conducted to find Young's modulus of CTD-101K-copper composite at liquid nitrogen temperatures. Work included design of a fixture for cantilever beam bend test on MTS -801 machine. Strain measurements were done using strain gauges.

3. EXPERIMENTAL METHODS AND MATERIALS

3.1 CURE INDUCED STRESS TEST (CIST):

Throughout the entire study, a stress monitoring technique developed at UT composites lab, the Cure Induced Stress Test (CIST), has been used. It uses a computer program which runs according to the cure cycle specified. The schematic of the test setup is shown in Figure 3.1. The fiber is placed between a fixed support and the load cell tip. It passes through two narrow slots made to the heating chamber .The silicone mold is placed at the center of the table. It has a slot on it through which the fiber passes. The wall thickness of the silicone mold is small to minimize the effect of its volume change on the overall effect of stresses on the fiber.

A thermocouple is placed closely to the matrix. The fiber is glued using an adhesive. Before starting the program, it is pretensioned. The ceramic block is kept over the fiber with the fiber passing through the slots at both ends. The heater is placed over it and the polymer is cured around a pretension fiber. Detailed description of the experimental setup and validation can be found in [28].

3.2 IN-CURE VOLUME CHANGE MEASUREMENT:

The in-cure volume change data for 3501-6 taken from [29] was used in the current work. Volumetric dilatometer was used to measure the total volume changes in [29].

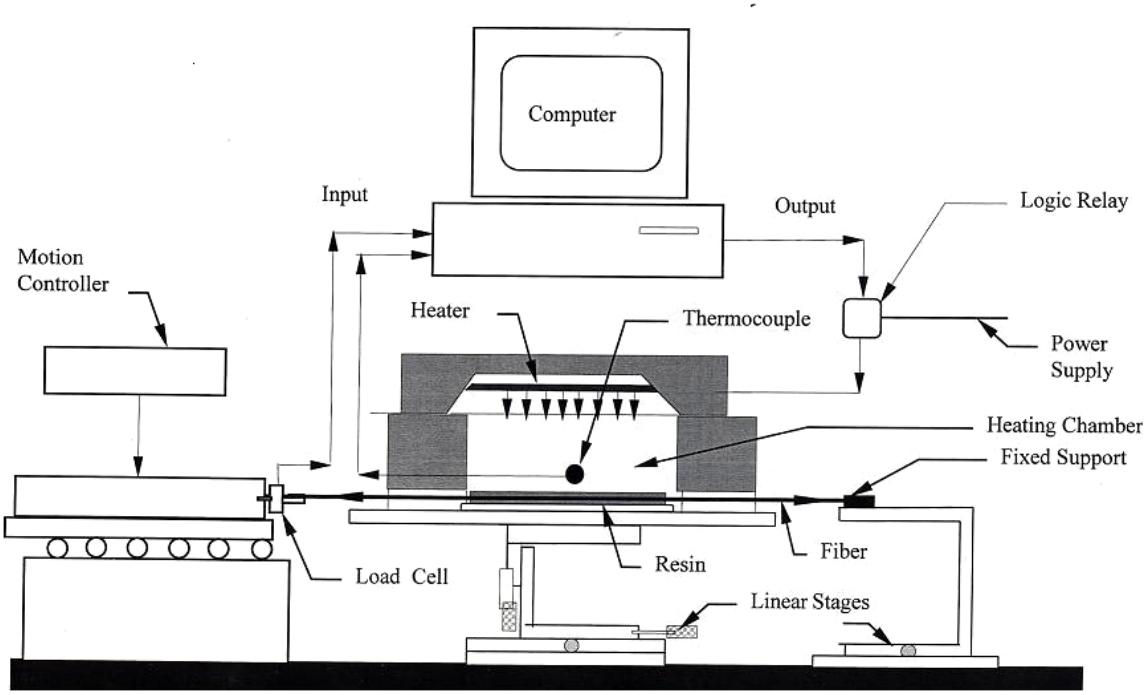

Fig 3.1: Schematic diagram of a single-fiber CIST setup

The Volumetric dilatometer used was the Gnomix Research PVT Apparatus. This instrument yields measurements of total sample volume change during a given cure cycle. The details of the experimental setup and procedure are explained in [31].

3.3 MATERIALS:

CTD-101K and CTD-404 are epoxide resins from Composites Technology Development Inc. The cure behavior study of these resins is important to know the scope for making optimal changes to the cure cycle. Their ease of handling, the stresses induced by them on the fibers during cure and cool down are some of the important factors in the selection of appropriate resin for modular coils. Both CTD-404 and CTD-101K, received as resin

and hardener, were mixed to proportions as recommended by the manufacturer. These resins are designed to work well at cryogenic temperatures. This is an important property required as cooling of the modular coils in QPS by liquid nitrogen is being considered.

The stresses induced by CTD-101K and CTD-404 on the fibers were determined from the CIST. The fibers used in this experimental study were copper and carbon-AS4. Standard cure cycle specified by the manufacturer was used to cure the samples of CTD-101K and CTD-404. The cool down data was recorded manually at the end of the cure cycle.

3.3.1 CTD-404:

CTD-404 was prepared from the resin and hardener supplied by Composite Technology Development Inc. The mixing proportion is 100 parts by weight of resin and 2.13 parts by weight of hardener. The resin, a solid at room temperature was heated to about 40 C. The resin, now in liquid state, was mixed with a viscous hardener in specified proportion. The resulting CTD-404 is liquid and doesn't require degassing. It was then immediately transferred into the silicone mold of CIST before it starts to solidify again.

3.3.2 CTD-101K:

CTD 101K is a modified anhydride cured epoxy system. It is available for CIST at UT composite slab. It was prepared by mixing part A (resin), part B (hardener) and part C (accelerator) as supplied in specified proportions. The mixing proportion is 100 parts by

weight of resin, 90 parts by weight of hardener and 1.5 parts by weight of hardener. The mixture is heated and stirred until a clear solution at 40-60 C is obtained. The mixture is now degassed at 27 in Hg for approximately 20 to 40 minutes until bubbles evolve infrequently from the mixture.

To find the modulus of the matrix, cured samples of CTD-101K and CTD-404 were made using the given cure cycles without the fiber reinforcement. Samples wide enough to fix strain gauges were obtained. A 3-point bend test was conducted on these samples. Modulus was determined using the strains obtained from the strain gauges. The young's modulus of CTD-404 was observed to be more than that of CTD-101. Tables 3.1 and 3.2 show the 3-point bend test data for the samples. The data from the tables was plotted in Figures 3.2 and 3.3. The slope from the plots was used in the calculation of elastic modulus. The modulus of CTD-404 using the data is 7.15GPa and that of CTD-101K is 4.54 GPa. The relatively higher young's modulus of CTD-404 over CTD-101K suggests that during cure it can induce more stresses on the reinforced fibers than CTD-101K. Higher cross link density of the polymer leads to its high elastic modulus.

3.3.3 Copper and Carbon Fibers:

The copper fibers were obtained from the stranded copper cable supplied. Copper fibers have an average diameter of 0.11 mm (approx). The diameter of the carbon fibers used varied from 8-10 micron. The young's modulus of copper fiber is 110 GPa and carbon fiber is 208 GPa.

Table 3.1: 3-point bend test data for CTD-404 sample

Load (N)	Strain x 1E-3
1	0.307
2	0.613
3	0.924
4	1.238
5	1.553
6	1.857

Table 3.2: 3-point bend test data for CTD-101K sample

Load (N)	Strain x 1E-3
1	0.837
2	1.682
3	2.525
4	3.34
5	4.2

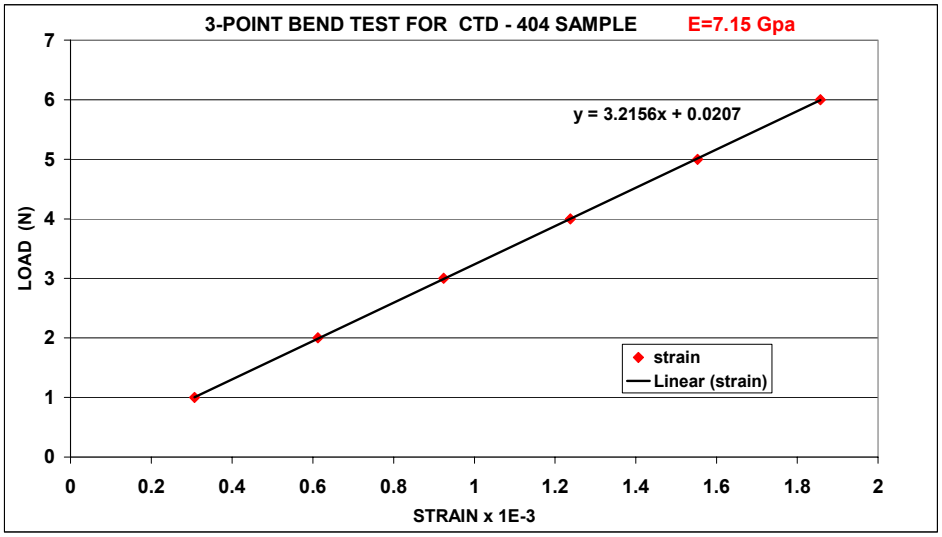

Fig 3.2: Strain data from 3-point bend test on CTD-404 sample.

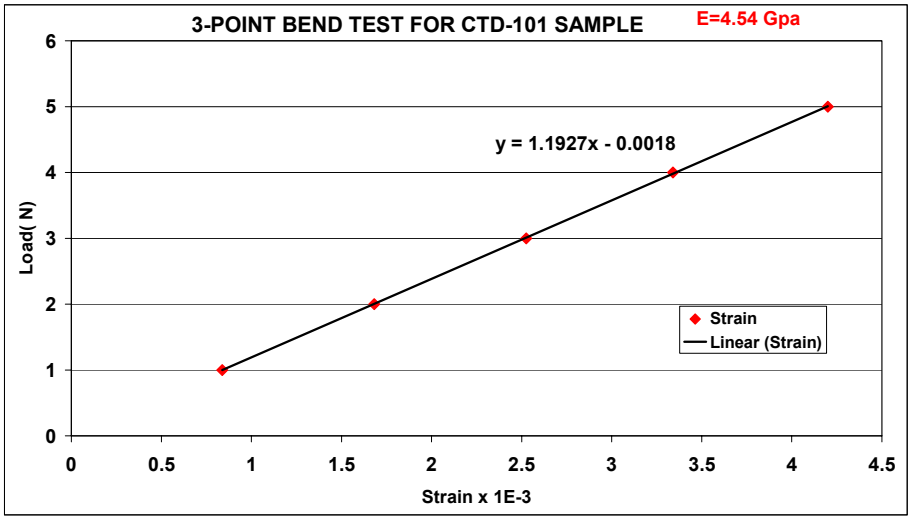

Fig 3.3: Strain data from 3-point bend test on CTD-101K sample.

The modulus of fiber is a factor which can affect the load on fiber. If the fiber has a higher modulus, more stress is required to strain the fiber. In other words, a fiber with higher modulus should show more increase in its load during cure than a fiber with lower modulus, provided the diameter of the fibers is same.

4. STUDY OF THE CURE INDUCED STRESSES ON COPPER AND CARBON FIBERS

The objective here was to study the general cure behavior of CTD-404 and CTD-101K, the stresses they induce on fibers and to minimize those stresses. CIST tests were run with CTD-404 and CTD-101K. The fibers were pre-tensioned before running the CIST. Initially the cure behavior of CTD-404 is described followed by CTD-101K.

4.1 CIST TESTS WITH CTD-404 AND FIBERS:

The standard cure cycle for CTD-404 is a 120 minute (2 hour) ramp from room temperature to 176 F, 960 minute (16 hour) hold at 176 F, 180 minute (3 hour) ramp from 176 F to 302 F and 240 minute (4 hour) hold at 302 F. Since copper has high coefficient of thermal expansion, the CIST data for CTD-404 –Copper experiment has the data of copper expansion included in it. To know the net effect of CTD-404 cure on the load of copper fiber, the copper fiber expansion data has to be subtracted from the original data. For this, a CIST test was run with copper fiber alone and no matrix surrounding it. The initial load of copper fiber in CTD-404-Copper experiment was adjusted to be close to the initial load of Copper fiber in this test for proper subtraction of copper expansion data. For carbon fiber, since its coefficient of thermal expansion is very low, a CIST test with carbon fiber alone was not necessary.

4.1.1 CIST with CTD-404 and Copper fiber:

Figure 4.1 shows the load change on pre-tensioned copper fiber during the time-temperature cycle used for the cure of CTD-404. Decrease in the load during the ramps is due to the copper fiber expansion. Copper fiber underwent creep during both dwells. During the first dwell, the load dropped initially and became constant towards the end of the dwell. During second ramp, the load continued to drop till the end of second dwell. The load increased during cool down as copper contracts and reached close to pre-tension load. Figure 4.2 shows a plot of load & temperature vs. time, from cured induced stress test with CTD-404 and copper fiber.

A drop in the copper fiber load during the initial ramp can be observed. This drop is due to the expansion of copper fiber. No drop in the fiber load, due to the flow of CTD-404 along the fiber, is observed, as CTD-404 is liquid when the CIST starts. With copper expansion included, the fiber seems to have experienced no stresses until the end of second ramp. During the dwell at 176F for 16 hr, the load dropped initially as the fiber underwent creep and became constant towards the end of dwell. The volume of CTD-404 started to shrink due to cross-linking during the second dwell of 4 hr at 302 F. The cross-linking continued gradually till the end of cure cycle, which can be observed from Figure 4.2. The increase in the load of fiber was observed from the start of the dwell to the end of the cure cycle. The cool down stresses induced by CTD-404 due to thermal shrinkage were more than the cure-induced stresses.

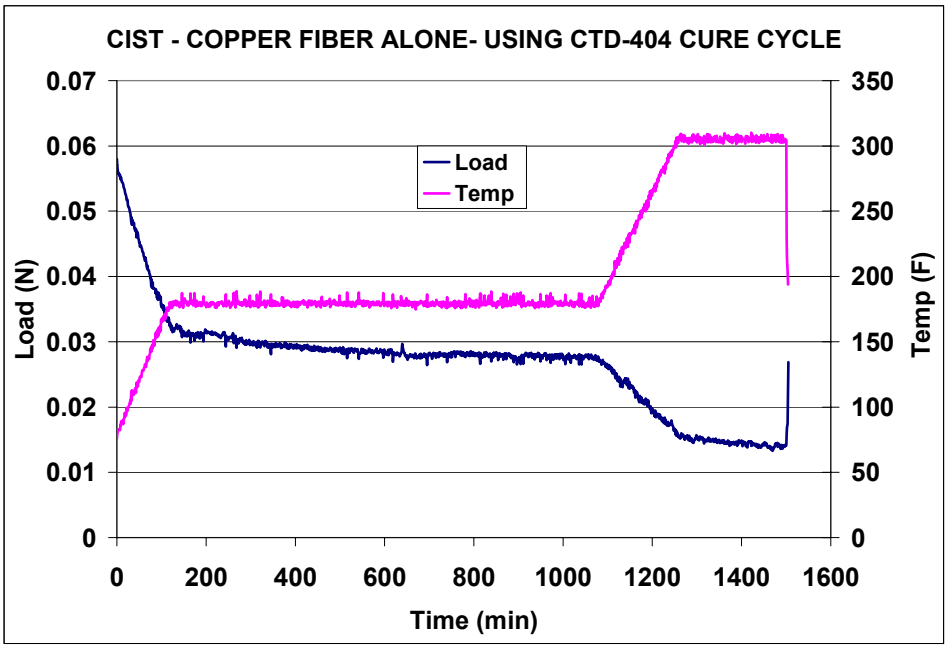

Fig 4.1: Fiber load change due to copper expansion: CTD-404 cure cycle

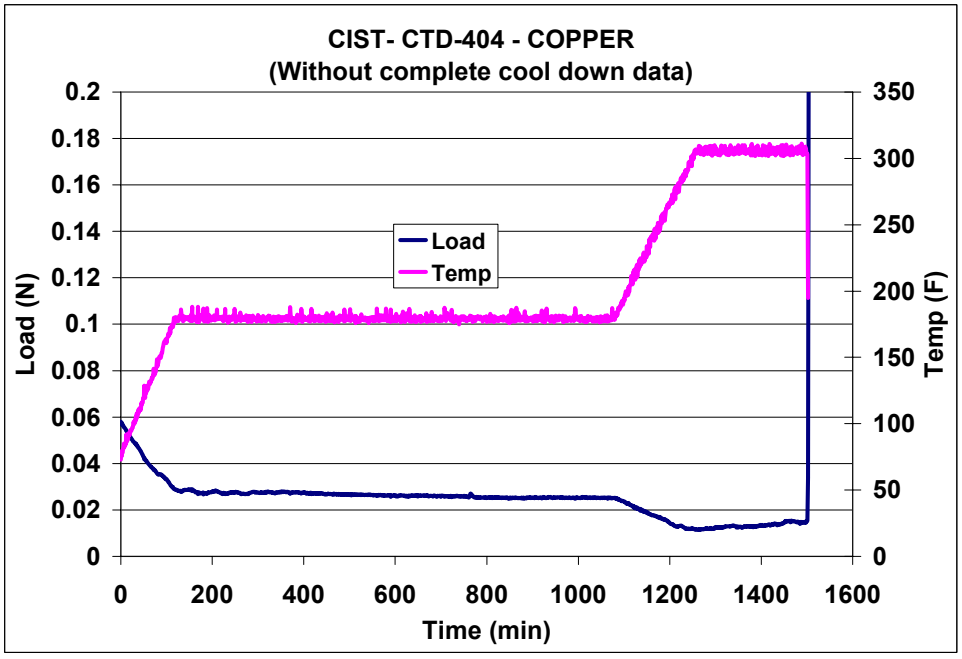

Fig 4.2: CIST data for CTD-404-copper fiber

The fiber load started to increase rapidly as soon as the cool down started. The initial load before the test was 0.0567 N and the load after complete cool down was above 1.552 N. Apart from the load due to copper contraction, the load increase was primarily due to the thermal shrinkage of CTD-404. Also since CTD-404 did not vitrify at the end of second dwell, cross-linking might have extended during the cool down, causing further stresses on the fiber.

As we have seen in section 3.3, the modulus of CTD-404 is relatively higher (7.15 GPa) than CTD-101K. During shrinkage it can induce more stress on the fiber for relatively less shrinkage. Also since the diameter of copper fiber is relatively large, the load is even higher due to greater surface contact with the matrix. Figure 4.3 shows the complete cool down data. For the last few minutes during the cool down, the data was arbitrarily taken as the fiber load exceeded the multi-meter range.

In order to determine the effect of only the matrix expansion and shrinkage during the cure cycle, the copper fiber load change due to thermal expansion and creep, shown in Figure 4.1, was subtracted from the copper fiber load change obtained from the copper/CTD-404 CIST experiment (Figure 4.2). The net effect of CTD-404 on copper is shown in Figure 4.4. The load change data during the cool down is not shown in Figure 4.4 because then the load axis scale will have to be large and the details of the curve during the cure cycle will not be clearly visible.

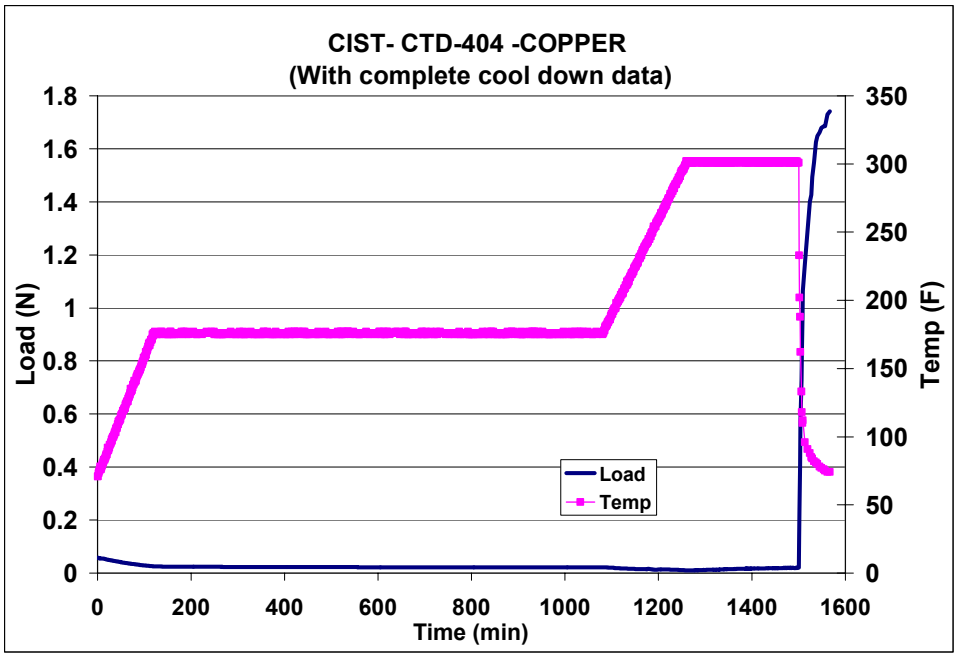

Fig 4.3: Copper fiber load increase during the cool down.

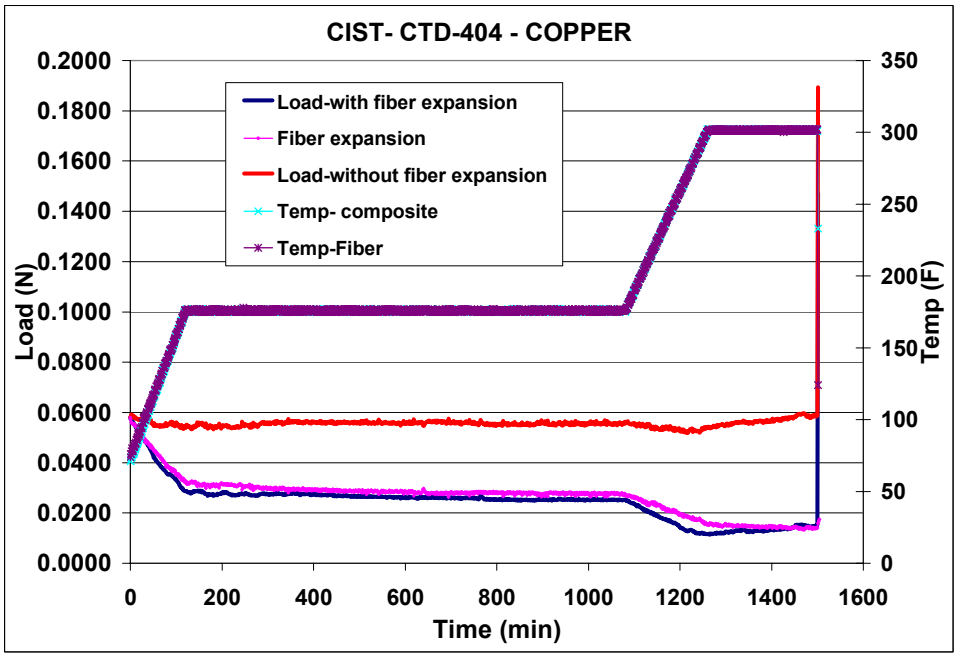

Figure 4.4: Fiber load data without copper expansion.

Red line denotes the net effect of CTD-404 on copper.

Till the end of the first dwell, there is no significant change in the fiber load. During the second ramp, a drop in the fiber load was observed. Simultaneous stress relaxation, due to temperature ramp, and cure shrinkage, due to cross-linking, might have occurred as the cure progresses causing less drop in the fiber load. During the last dwell of 4 hr there is a steady increase in the load, as the resin continues to cure with no increase in temperature. It can be observed that, if the second dwell were not terminated after 4 hrs, the cure would have progressed causing more cross-link density, hence more volume shrinkage leading to more stresses on the fiber. The cure would have stopped when the resin got vitrified. As we know the elastic modulus of CTD-404 is 7.15 GPa (section 3), it appears the second dwell duration was sufficient to obtain a stiffer CTD-404, as the cross-linking would still have extended during the cool down.

Overall the cure stresses of CTD-404 are relatively less, which can be due to 25 hr long cure cycle time. But the cool down stresses are high which can lead to significant warpage.

4.1.2 CIST with CTD-404 and Carbon Fiber:

To verify and compare the net effect of CTD-404 on reinforced fiber, a CIST was run with CTD-404 and carbon fiber. The stress profile on the carbon fiber from CIST is shown in the Figure 4.5. The plot looks similar to that of the net effect of CTD-404 on copper, which is expected. Initially a negligible drop of 0.002N in the carbon fiber load was observed which could be an experimental fluctuation. The carbon fiber load remained constant till the end of the first dwell. The load increase during the second

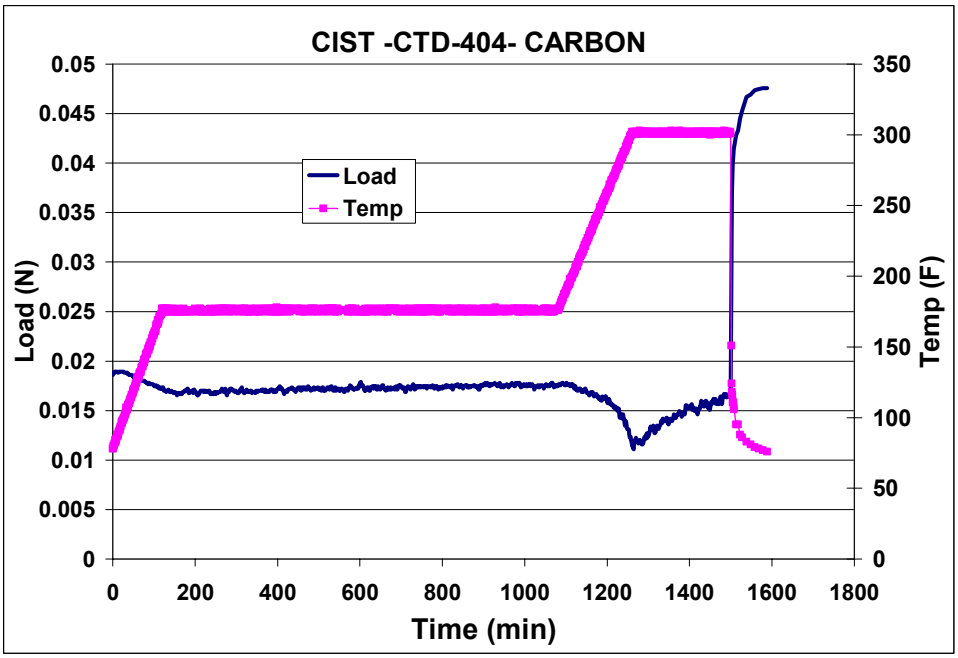

Fig 4.5: Carbon fiber load data for CIST on CTD-404

dwell can be observed as the CTD-404 continues to cure to the end of cure cycle. As the thermal expansion of the carbon fiber is negligible, no data was subtracted from the composite load data. While the load profile of carbon fiber (Figure 4.5) looks similar to that of copper (Figure 4.4), the amount of load on copper is much higher owing to the larger diameter of copper. However, for carbon fiber even with a much smaller diameter (8 microns), significant stress was observed on the fiber owing to the high stiffness of CTD-404 and that of carbon fiber. Here too, the increase in the fiber load from the start of cool down to the end of cool down was found to be very high. This is due to the thermal shrinkage of CTD-404 during cool down, which is more than the cure shrinkage. Also, since CTD-404 did not vitrify at the end of second dwell, cross-linking might have progressed during cool down causing further increase in the fiber load.

4.2 CIST TESTS WITH CTD-101K AND FIBERS:

The standard cure cycle of CTD-101K used is a 10 min ramp to 230 F, 5 hr stay at 230 F, 10 min ramp to 257 F, Post Cure for 16 hr at 257 F and cool down. Here too the copper expansion data from the CTD-101K-Copper CIST has to be subtracted to know the net effect of CTD-101k on copper fiber. For this, a CIST test was run with copper fiber alone and no matrix surrounding it. The initial load of copper fiber in CTD-101K-copper experiment was adjusted to be close to the initial value of copper fiber in this test for proper subtraction of copper expansion data. CIST for carbon fiber alone without matrix was not run, as there was no thermal expansion of carbon fiber.

4.2.1 CIST with CTD-101K and Copper-Fiber:

Figure 4.6 shows the load change on the pre-tensioned copper fiber during the time-temperature cycle used for the cure of CTD-101K. Owing to higher coefficient of thermal expansion of copper, we can see a significant drop in the load of copper fiber during the initial ramp and a small drop during the second ramp as the temperature difference is less between the first and second ramps. During the first and second dwell, there is a small drop in the fiber load initially, as the fiber underwent creep. This data was subtracted from the composite data to see the net effect of CTD-101K on copper. Figure 4.7 shows the copper fiber load profile for CIST on CTD-101K. The load drop during in the initial temperature ramp is a result of both thermal expansion of copper and the flow of viscous CTD-101K.

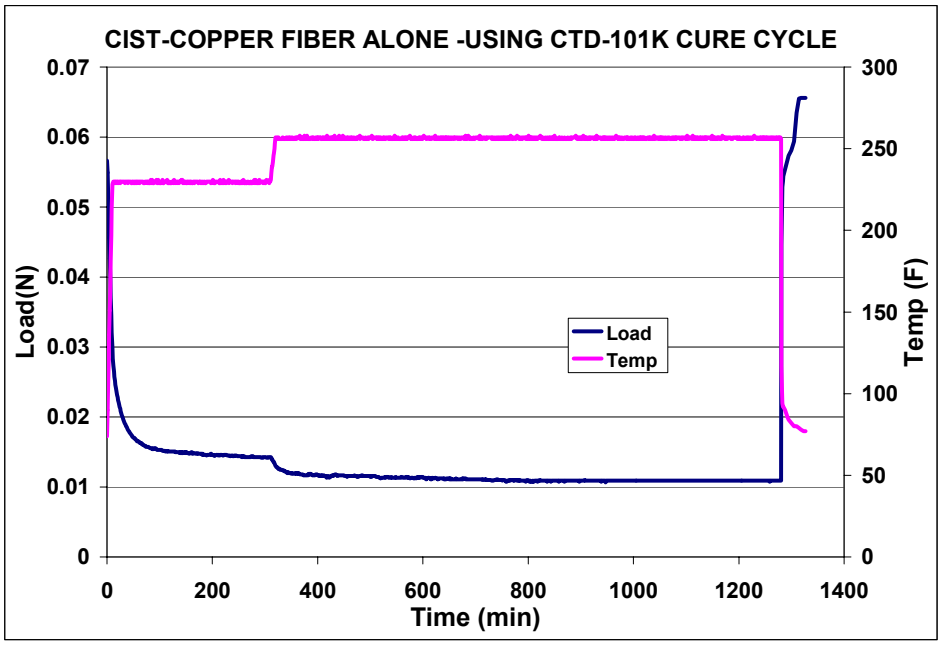

Fig 4.6: Fiber load change due to copper expansion: CTD-101K cure cycle

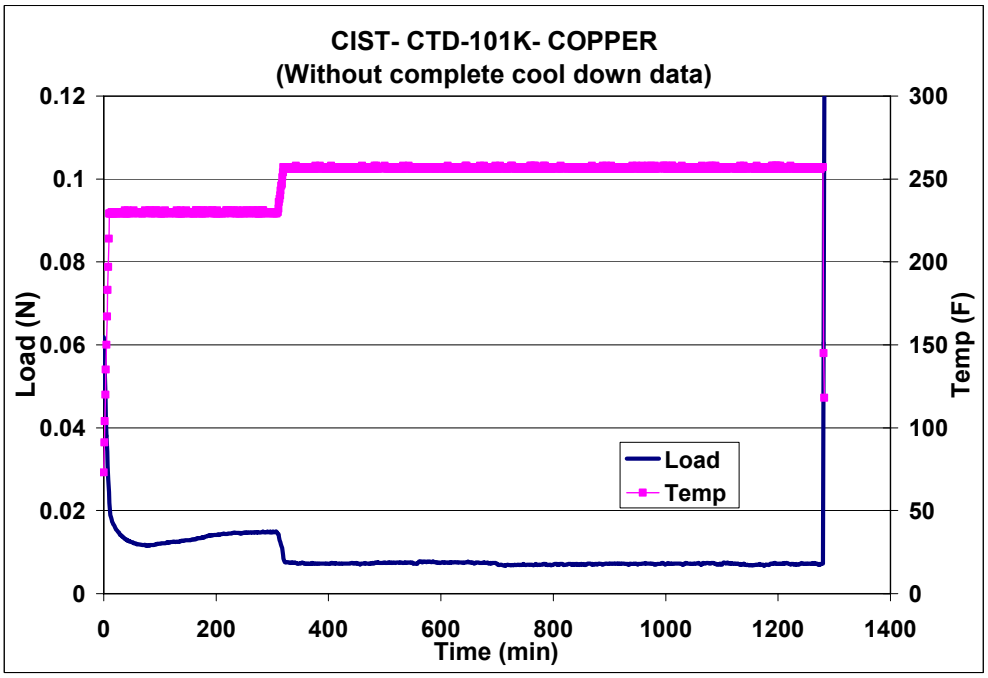

Fig 4.7: Load profile of copper fiber for CIST on CTD-101K

Also, uncured CTD-101K is more viscous at room temperature compared to CTD-404, which is almost liquid at room temperature. The viscous liquid when poured in the silicone mold, the fiber running through the mold is pulled down increasing the load on the fiber. When heated during the ramp, the viscous CTD-101K starts to expand and flow initially, and during this the load on the fiber gets released. This drop in the load happens during the first ramp. During the first temperature hold, the load of copper fiber steadily increases. The load became constant towards the end of first dwell as the polymer gets vitrified. During the post cure time of 960 minutes (16 hr), no significant cure stresses were observed. Post cure is done to extend the cure and to remove any volatile matter left in the polymer. The relatively low curing stresses on the copper fiber may be due to low cross-link density compared with CTD-404, which can be inferred from the modulus data in Section 3.2.

The cool down stresses were observed to be high, owing to the thermal shrinkage of the matrix and the larger diameter of the copper fiber. Figure 4.8 shows the load profile of copper fiber during cool down. The load data of copper fiber due to its expansion during the cure cycle, shown in Figure 4.6 was subtracted from the composite to see the net effect of CTD-101K on copper. Figure 4.9 shows the resulting curve. As explained in 4.2.1, a drop in the copper fiber load during the initial ramp was observed as the matrix flows along the fiber releasing the fiber load. Also the pulled fiber gets released as the matrix flows dropping the load further. During the 300-minute (5 hr) dwell, CTD-101K continues to cure and gets vitrified towards the very end of the dwell. The resin is then post cured for 16 hr. No significant fiber load change was observed during post cure.

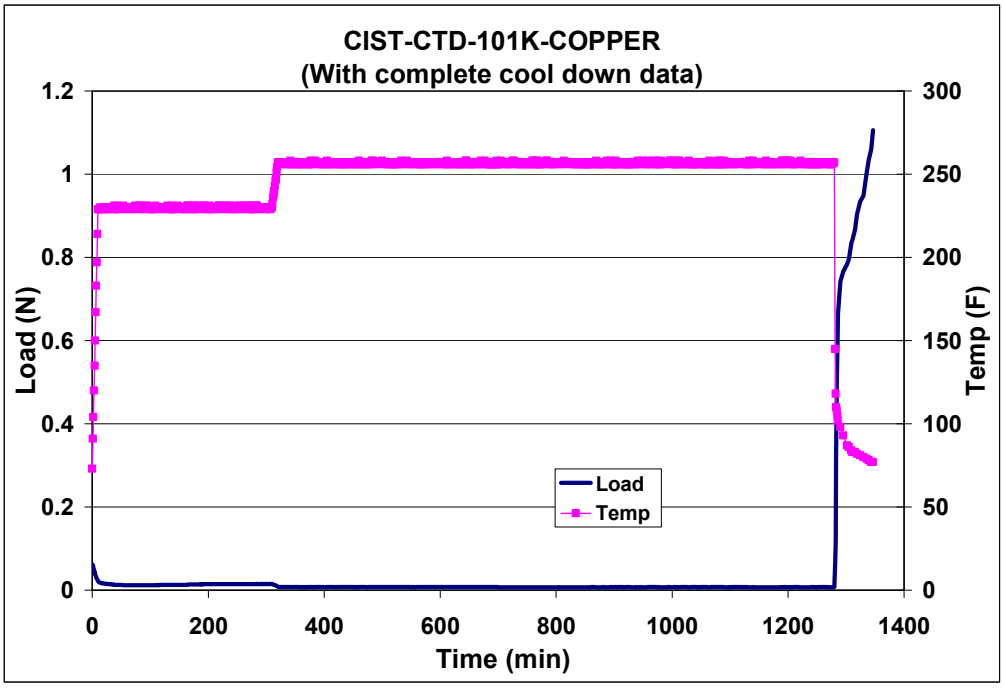

Figure 4.8: Copper fiber load profile with complete cool down data.

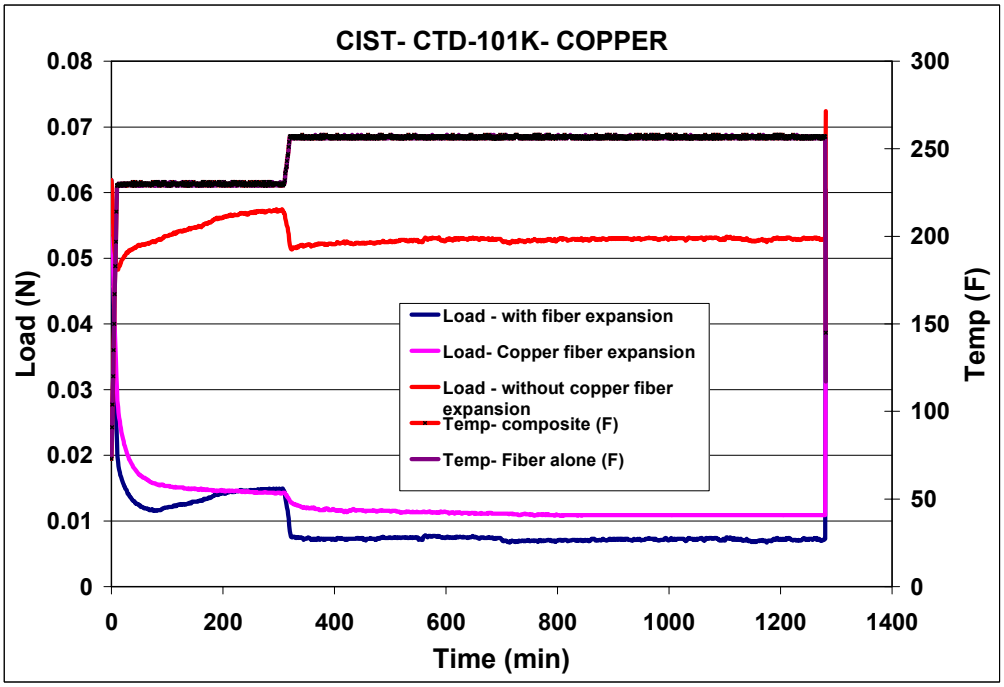

Fig 4.9: Load data of copper fiber without fiber expansion.

A possible explanation for this may be that the increase to post cure temperature was not sufficient for the polymer to continue further cross-linking. Overall, the cure-induced stresses are low for CTD-101K, which can be due to 21 hr long cure cycle.

4.2.2 CIST with CTD-101K and Carbon Fiber:

To verify and compare the net effect of CTD-101K on reinforced fiber, a CIST was run with CTD-101K and carbon fiber. Figure 4.10 shows the load profile carbon fiber for CIST on CTD-101K. As expected, the plot looks similar to the plot for net effect of CTD-101K during the cure. The load drop during the initial ramp is less for carbon fiber owing to its very small fiber diameter (8 microns) compared to that of copper (0.11 mm).

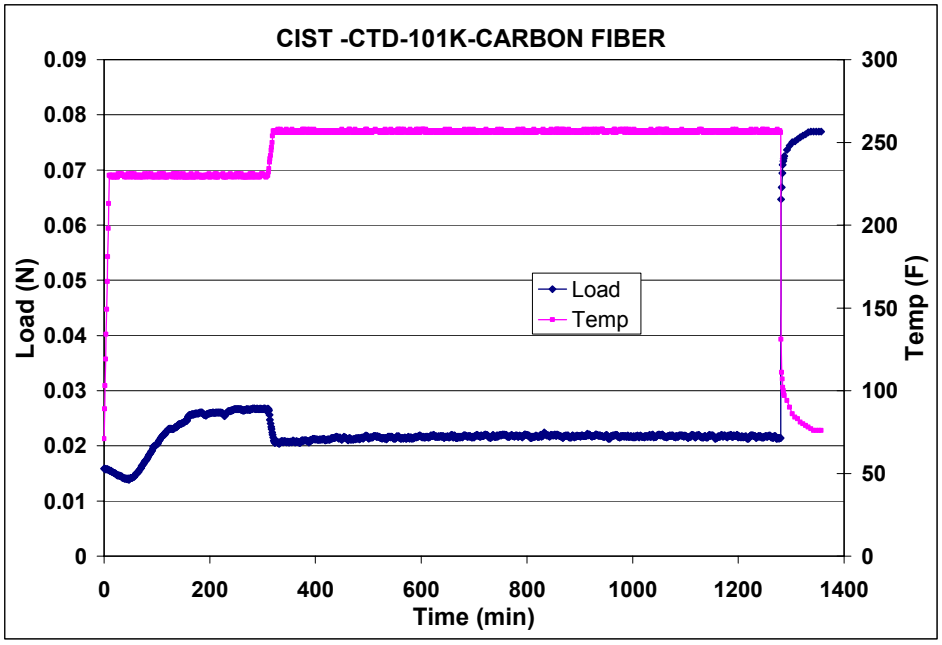

Fig 4.10: Load data of carbon fiber for CIST on CTD-101K

The load increased during the dwell till the end of cure cycle. The load became constant towards the end of first dwell as the polymer got vitrified. The load due to the thermal shrinkage during cool down was high. However, for carbon fiber even with a much smaller diameter (8 microns), significant stress was observed on the fiber owing to the high stiffness of CTD-101K and that of carbon fiber.

4.3 COMPARISON OF CTD-404 AND CTD-101K:

A comparison of CTD-404 and CTD-101K is presented in Table 4.1. It briefly summarizes the overall study of cure behavior of CTD-404 and CTD-101K. Both CTD-404 and CTD-101K have relatively low cure stresses and high cool down stresses.

Table 4.1: Comparison of CTD-404 and CTD-101K

Property	CTD-404	CTD-101K	Comments
Components	**Resin :** 100 parts by weight **Hardener :** 2.13 parts by weight	**Resin:** 100 parts by weight **Hardener:** 90 parts by weight **Accelerator:** 1.5 parts by weight	CTD-404 components are easier to mix compared to CTD-101K
Degassing	Not required	Required	C TD-404 is liquid after mixing.
Cure Cycle	2h ramp from room temperature to 80 C, 16 h hold at 80 C, 3h ramp from 80 C to 150 C, 4h hold at 150 C	10 min ramp to 110C, 5 h hold at 110 C, 10 min ramp to 125C, post cure 16 h hold at 125 C	Both have long cure cycle times. CTD-404 cure cycle (25 hr) is longer compared to CTD-101K (21 hr).
Young's Modulus	7.15 GPa.	4.54 GPa	Indicates higher cross-link density for CTD-404.
Ease of Handling	Easier	Easy	CTD-404 doesn't require degassing, has only two parts to mix, and is liquid at room temperature.
Cure Induced Stresses	less	Lesser	Stresses induced by CTD-101K were lesser than CTD-404 because of its lower cross-link density compared to CTD-404.
Stresses due to thermal shrinkage during cool down	Higher	High	Higher for CTD-404 than CTD-101K due to higher cross-link density.

5. CHARACTERIZATION OF ELASTIC MODULUS DEVELOPMENT OF 3501-6 DURING CURE

The objective of the work was to characterize the elastic modulus development of CTD-101K and CTD-404 during cure. As will be shown in 5.1, the approach requires fiber-load data and in-cure volume change data. The fiber-load data for CTD-101K and CTD-404 can be obtained from CIST. But since the volumetric dilatometer, required to get the in-cure volume change data for CTD-101K and CTD-404, was not available, the available data of in-cure volume changes and fiber-load during different cure cycles for 3501-6 was used for the work [29].

5.1 APPROACH

This study describes a new approach to determine the polymer modulus development as it cures. The modulus development was characterized based on the difference in the linear displacements of the polymer during cure without a fiber and with fiber reinforcement. Introduction of new covalent bonds during polymerization reduces the average atom distances resulting in polymer shrinkage. Flow of the polymer can occur before gelation but is restricted thereafter. This shrinkage due to the restricted flow of polymer and the presence of fiber leads to stress buildup. The presence of fibers in the polymer constrains the polymer volume change. Hence there is a difference in the displacements of the polymer when there is no fiber and when there is fiber

reinforcement. In this study the difference is assumed to be directly proportional to the modulus development of the polymer. The stresses produced on the fiber due to polymer volume change are dependent on the difference in the polymer volume change (i.e. difference between the polymer volume change with and without the fiber) and the instantaneous stiffness of the polymer. Stresses produced on the fiber are not large enough to cause slip at the interface during the entire cure cycle [30]. Hence the shrinkage of the polymer during cure is assumed to be equal to the change in length of the fiber between load cell and outside the polymer. Stress relaxation during cure was not taken into account.

5.2 RESULTS AND DISCUSSIONS

The elastic modulus development was characterized for 136 C and 169 C isothermal cure cycles. The volume change data from the volumetric dilatometer and the fiber-load data from the Cure Induced Stress Test were obtained from previous work [27], plotted in Figures 5.1 and 5.2. The polymer specific volume change data was obtained from volume change data.

5.2.1 Linear Displacement of 3501-6 from Volumetric Data

The expression for linear strain from volumetric data was taken from [29]. The expression gives linear strain in terms of volumetric strain.

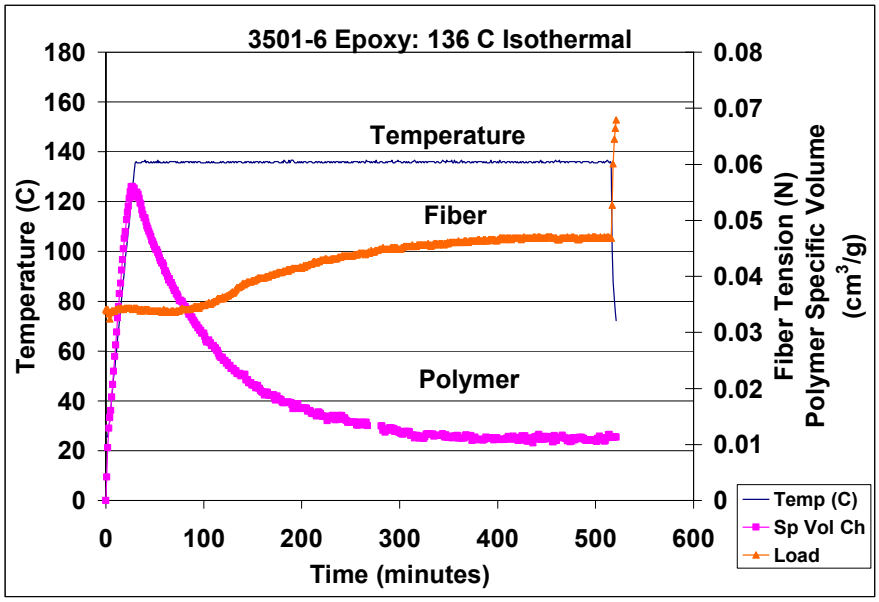

Fig 5.1: Polymer volume changes and fiber tension results during 136C isothermal cure cycle.

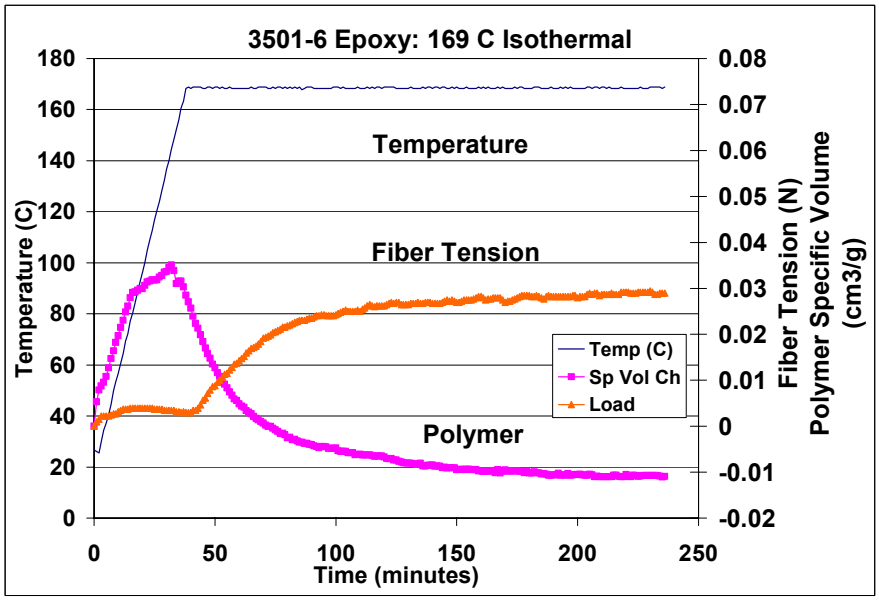

Fig 5.2: Polymer volume changes and fiber tension results during 169 C isothermal cure cycle

v_0 = Original specific volume

Δv = Change in specific volume.

ε_{vol} = Volumetric strain.

ε = Linear strain.

$$\varepsilon_{vol} = \frac{\Delta v}{v_0}$$

$$\varepsilon = (1 + \varepsilon_{vol})^{1/3} - 1$$

v_0 -The original specific volume is calculated from the dimensions of sample used in Cure Induced Stress Test (CIST). The volumetric strain ε_{vol} and the linear strain ε were obtained from the above relation. The linear displacement of the polymer without fiber was obtained from the linear strain of half the length of the specimen. The displacement values were calculated from the data taken after the polymer developed sufficient stiffness, ahead of its gel point. Stress-relaxation during the temperature ramp and absence of cross-link network over the entire polymer before it develops stiffness results in polymer flow over the fiber. The time, at which the rate of polymer volume change decreases was taken from the plot, approximately at a time when the load on the fiber has a marked increase. The displacement obtained at this time is a result of flow of the polymer along the fiber. Hence the initial value of displacement calculated at that time is set to zero. The values at all the time steps, till the end of cure cycle, were taken as the difference of the initial and current values, giving absolute displacement of polymer without fiber reinforcement after the polymer develops sufficient stiffness.

5.2.2 Change in Length of fiber due to Cure Induced Stress :

Due to the constraint provided by the fiber, the polymer in the vicinity of the fiber should shrink less compared to polymer away from fiber. However, for simplicity, uniform shrinkage over entire length was assumed. The fiber from the load cell tip to the polymer is strained due to tension. The tension along the fiber axis is caused by the shear stress on the fiber inside the polymer. The linear displacement of polymer due to shrinkage, with fiber reinforcement, equals the change in length of the fiber, from load cell tip to the polymer. The displacement of the fiber was determined using the relation

$$\delta = \frac{PL}{AE}$$

Where P = Load on the fiber in Newton

L = One-half the length of the fiber outside the polymer

A = Area of cross-section of the fiber

E = Young's modulus of the fiber.

The displacements of the fiber were calculated at each time step from the point where the fiber load has a marked increase to the end of cure cycle. Since the fiber is already in pretension, the value represents the displacement due to pretension and due to the cure shrinkage of the polymer. Hence the displacement value for the first data time was set to zero. The absolute values of displacements at all the time steps till the cure time were obtained as the difference of the displacement at that time and the initial displacement

value due to pretension. These values of displacement of the fiber equal the linear displacement of the polymer with fiber reinforcement.

5.3 DIFFERENCE IN DISPLACEMENTS OF 3501-6:

As shown above, the 3501-6 polymer volume displacement with and without fiber reinforcement was obtained. At each time step, the difference of the displacement values was recorded. The difference in displacement values were plotted versus time as shown in figure 5.3 and 5.4. When the plot is compared with fiber tension profile in figure 5.2, it was observed that the difference in displacements curve mimics the progression of the cure of polymer and hence the development of polymer modulus.

5.4 MODULUS CHARACTERIZATION:

As the polymer cure progresses, the cross-links continue to develop over the entire polymer increasing its stiffness. Increased stiffness leads to increased load on the fiber. As shrinkage in the polymer and its instantaneous stiffness are the only factors producing stresses on fiber, proportionality can be assumed between the polymer volume displacement and modulus developed. Here a direct proportionality was assumed between the difference in displacements of the polymer volume, with and without fiber reinforcement, and the modulus. The plots in Figure 5.3 and 5.4 were used to characterize the modulus development of polymer during cure. Samples, partially and completely cured, were made to get the experimental modulus values during and after complete cure.

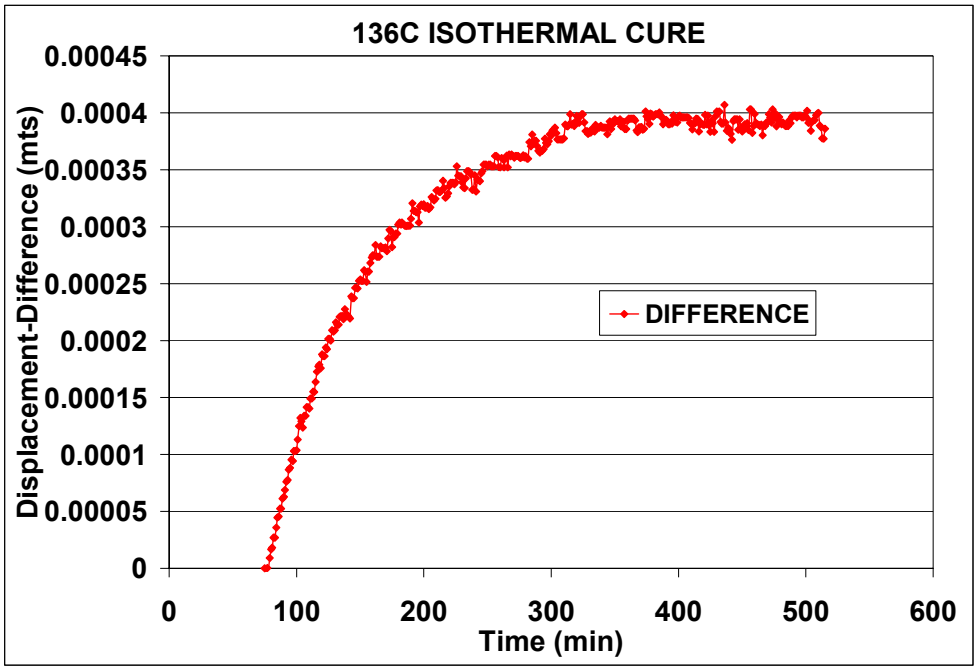

Fig 5.3: Plot for difference in displacements vs. Time: 136 C isothermal.

Displacement-Difference in the plot denotes the difference in the polymer volume displacement with and without the fiber. The difference increases as the polymer cures mimicking the fiber load increase and the degree of cure.

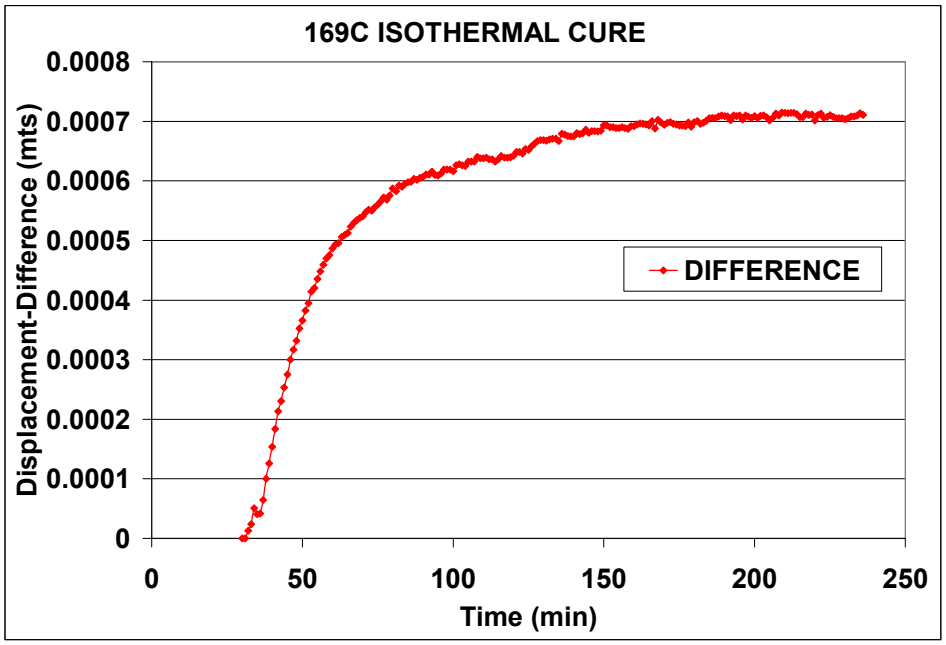

Fig 5.4: Plot for difference in displacements vs. Time: 169 C isothermal.

Displacement-Difference in the plot denotes the difference in the polymer volume displacement with and without the fiber. The difference increases as the polymer cures mimicking the fiber load increase and the degree of cure.

The samples were made in sizes suitable for mechanical testing. Strain gages were glued and three-point tests were performed on the samples to obtain the elastic modulus values at different cure times [27]. Two experimental modulus values for each isothermal cure cycle were available in literature. One value was used to scale the difference in displacement plots. The other experimental value was used to verify the plot. The plots were scaled separately for each isothermal cure cycle. *Diff* in the plot denotes the scaled data of the modulus from the difference in displacements data.

For 136 C isothermal (Figure 5.5), modulus value at 480 minutes was used to scale the plot. The modulus value at 210 minutes was used to verify the scaled plot. Note that the value at 210 minutes falls on the curve. A slightly higher value could be expected from the three-point bend test as the modulus value was obtained after the partially cured sample was allowed to complete cool down. But as the cure temperature, 136 C, is less than the standard cure temperature, 177 C, the cross-links do not extend much during the cool down.

For 169 C isothermal (Figure 5.6), modulus value at 180 minutes was used to scale the plot. The value at 45 minutes was used to verify the curve. As expected the modulus would not fall on the curve but shoots higher. This is due to the higher temperature of the cure cycle, 169 C, which is closer to the standard cure temperature of the polymer, 177 C. Hence polymer may continue to cross-link even during the cool down. Therefore the experimental value of partially cured samples is higher than the value predicted from our

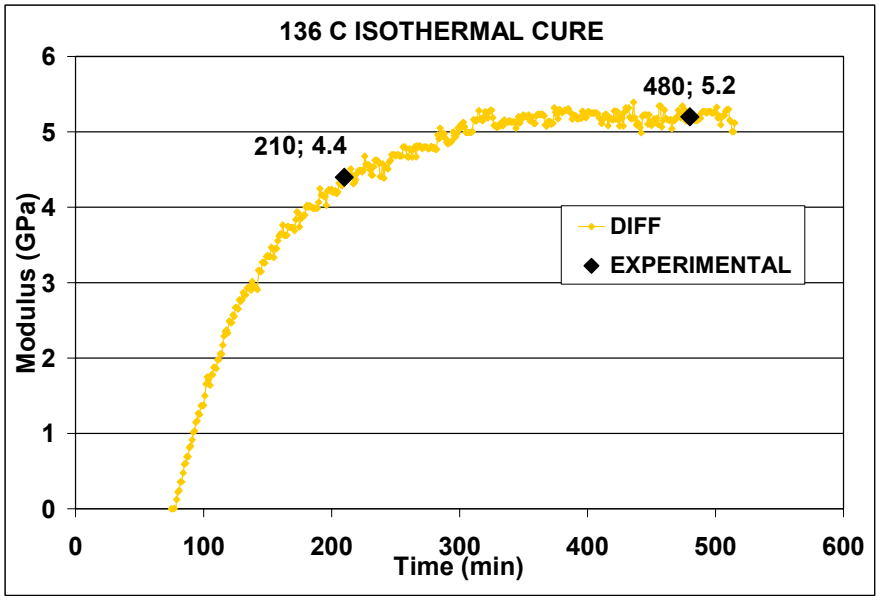

Fig 5.5: Scaled plot of difference in displacements for elastic modulus Characterization. : 136C isothermal

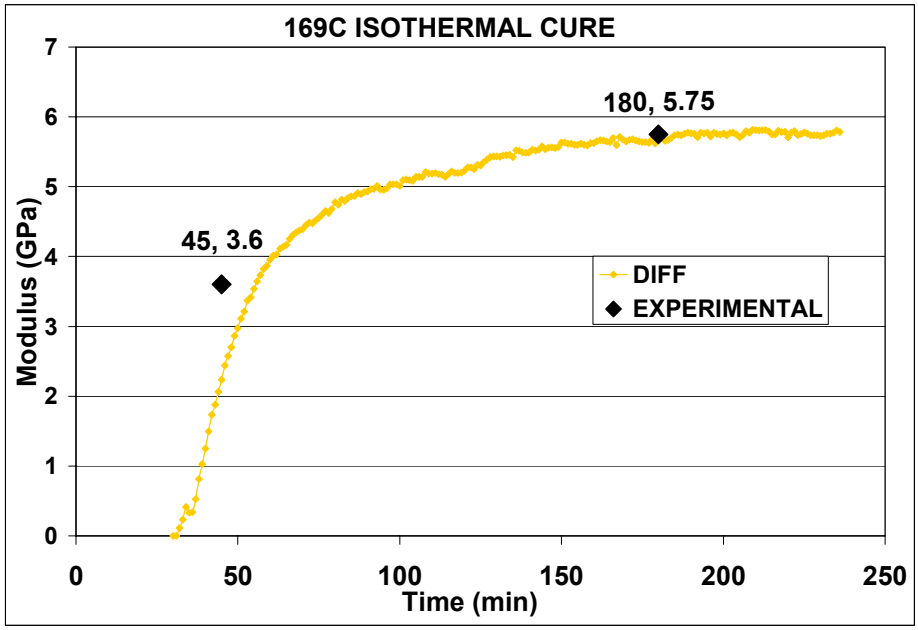

Fig 5.6: Scaled plot of difference in displacements for elastic modulus Characterization. 169 C isothermal

method. Further calibration was performed using the modulus values during cure, available in literature [30], shown in figure 5.7 and 5.8.

The modulus values from literature for 136 C isothermal fall on the curve. The values for 169 C isothermal slightly overshoot the curve initially and fall on the curve later towards to the end of cure. The method was developed for isothermal cure cycles but it can also be applied to multi ramp cure cycles, as the cure process is same.

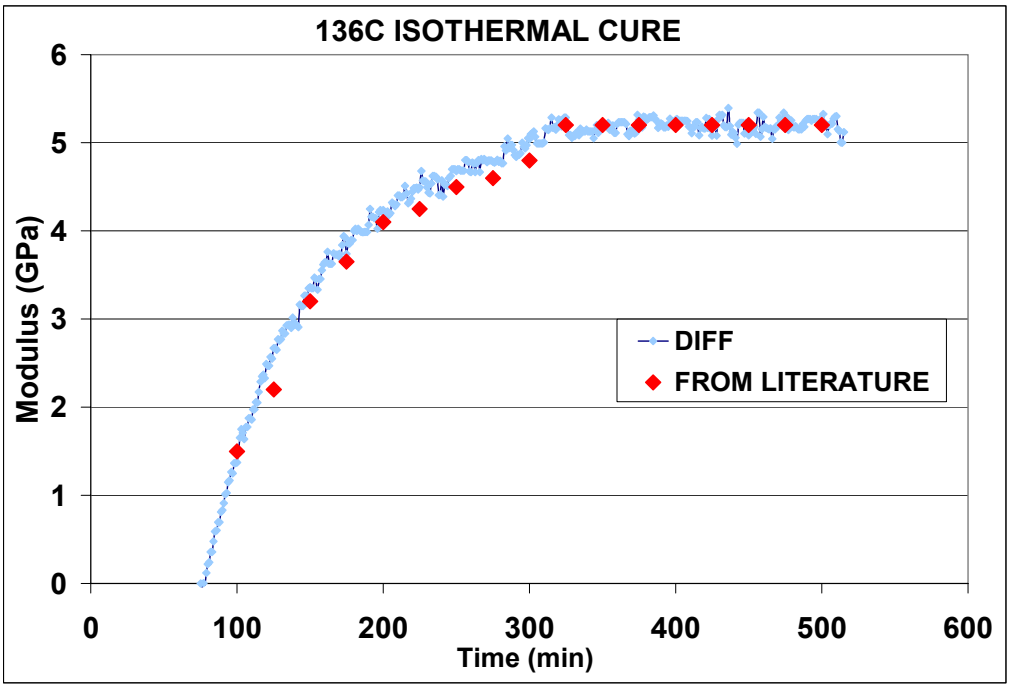

Fig 5.7: Calibration of Modulus characterization plots with data available in literature: 136 C isothermal

Diff denotes the scaled data of the modulus from the difference in displacements data.

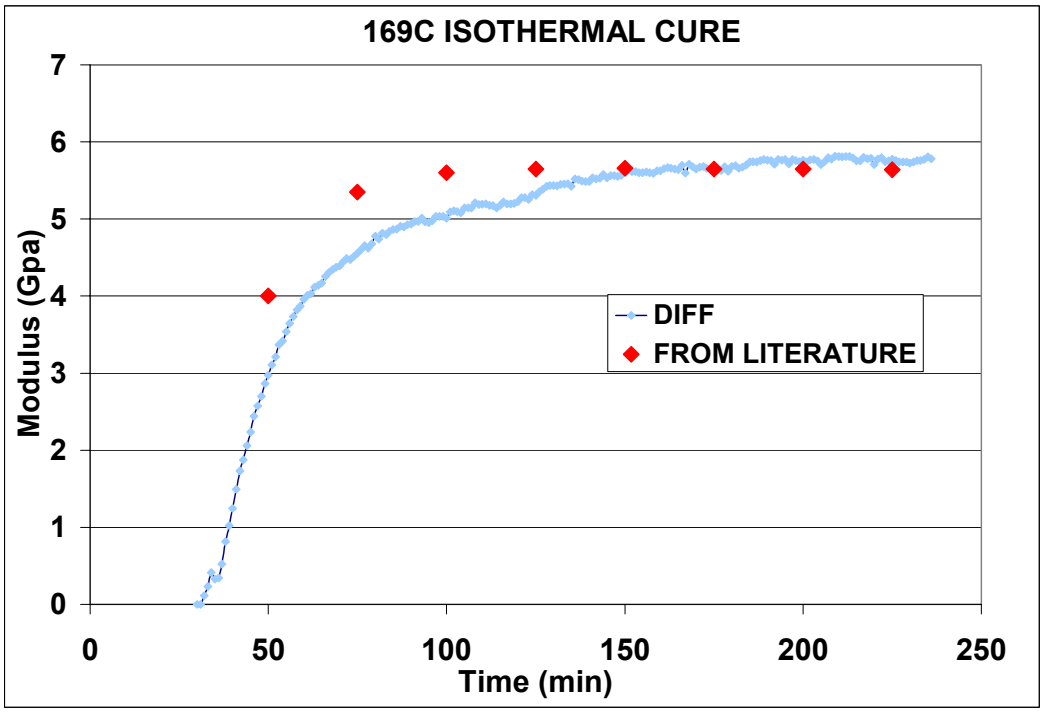

Fig 5.8: Calibration of Modulus characterization plots with data available in literature: 169 C isothermal.

Diff denotes the scaled data of the modulus from the difference in displacements data.

6. DETERMINATION OF ELASTIC MODULUS OF CTD-101K-COPPER COMPOSITE IN LIQUID NITROGEN

6.1 NEED FOR LOW OPERATING TEMPERATURES FOR THE COILS:

In an operating fusion reactor, part of the energy generated will serve to maintain the plasma temperature as fresh deuterium and tritium are introduced. However, in the startup of a reactor, either initially or after a temporary shutdown, the plasma will have to be heated to 100 million degrees Celsius.

In current tokamak, QPS and other magnetic fusion experiments, insufficient fusion energy is produced to maintain the plasma temperature. Consequently, the devices operate in short pulses and the plasma must be heated afresh in every pulse.

The pulse length depends on the operating temperature of the coil set, the current density in the copper, and the voltage available from the power supplies. Low temperature operation of the coils helps in increasing the current density and the pulse length. The modular coil windings can be cooled with room temperature gas, but additional performance is possible by using refrigerated gas below room temperature. Figure 6.1 illustrates the dependence of pulse length on coolant schemes, including cryogenic cooling, and on current density.

A flattop time of at least ~0.5 s is needed to allow time for eddy currents in conducting structures (the aluminum vacuum tank and the coil cases) and plasma currents (bootstrap

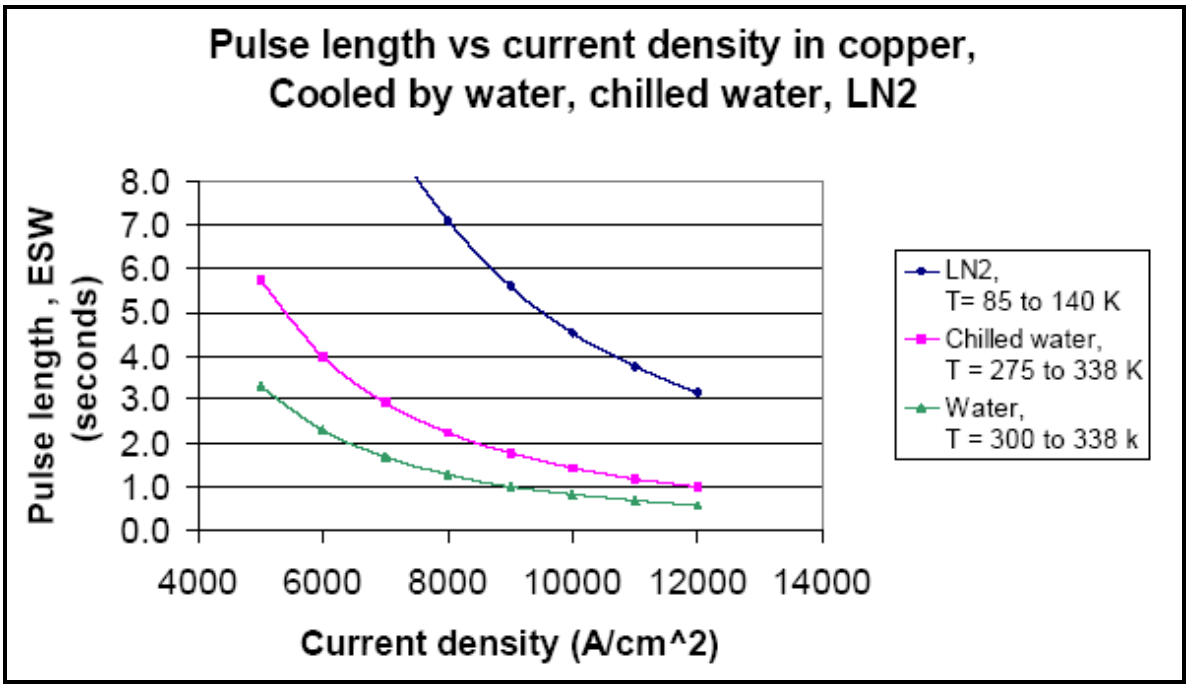

Fig 6.1: Pulse length vs. Current density in copper for various coolants.

(Longer pulse lengths (8 sec) from cooling with LN2)

and Ohmic) to come to equilibrium and to keep the temperature rise in the modular coil conductor to a reasonable value

Since the coils are located in a vacuum, they can be operated over a wide range of temperatures. As illustrated in Figure 6.2, reducing the temperature only slightly below room temperature can have a marked effect on the flattop time, and taking the coils to cryogenic temperatures enables flattop times of several seconds.

Owing to the advantages of LN2 as coolant, the mechanical properties of the coil have to be verified at that temperature. Here the objective is to find the young's modulus of copper-CTD-101K composite bar at room temperature and at liquid nitrogen temperature.

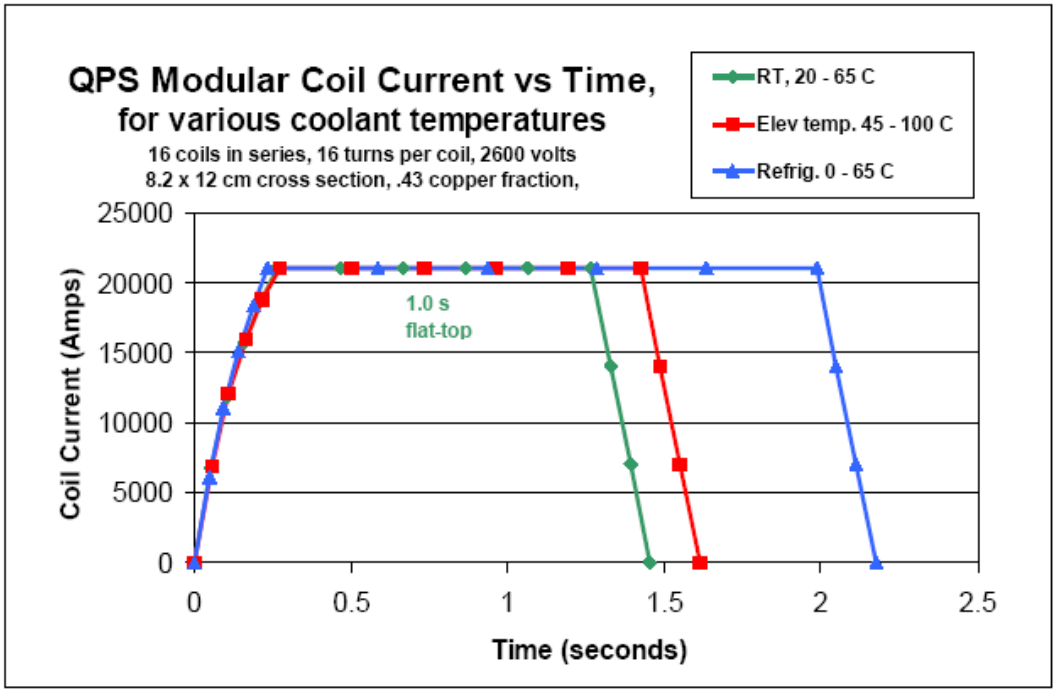

Fig 6.2: QPS coil current vs. time

(Increase in the flattop time from 1 sec to ~ 2 sec as the coolant temperature drops from 45-100C to 0-65C)

6.2 EXPERIMENTAL:

The Elastic Modulus of copper-CTD-101K composite in liquid nitrogen was found by performing a cantilever beam bend test on a MTS 810 machine.

6.2.1 Preparation of Test Piece:

As shown in Section 1.3 that in the construction of coils, there are two layers tightly wrapped on the composite, glass cloth and glass cloth co-wound with kapton. Both these

layers were removed prior to the testing. Strain gages from Vishay Measurements, which work at cryogenic temperatures, were used. A pair of strain gages was fixed on both the top and bottom of the composite bar. This helped to get the strain data simultaneously for tension and compression for the cantilever bend test. The strain gages were connected to the signal conditioning amplifier with wires. Figure 6.3 shows a photograph of the composite bar with strain gages.

6.2.2 Design of Fixture:

A fixture was required to perform the cantilever bend test on MTS machine. The fixture was needed in a way where it can hold the composite piece and contain the liquid nitrogen. Keeping these requirements in view, a fixture was designed and fabricated at

Fig: 6.3 Copper-CTD-101K composite bar with strain gages.

UT workshop to perform the cantilever bend test. The engineering drawings of the fixture and the loading arm were shown in appendix. Figure 6.4 shows a photograph of the fixture. The fixture has a rectangular slot on the top, which has enough volume to immerse the composite bar in liquid nitrogen. It has a square hole through the left wall inside. From the top a threaded hole was drilled. A bolt through the threaded hole can hold the composite. A small rectangular metal piece was placed on the composite bar in the hole to tightly hold the bar with the bolt pushing from the top making it a cantilever. A metal plate was welded to the bottom of this fixture for gripping on MTS machine. The plate goes in between the jaws of the machine. A loading arm, which is a metal piece with a ring at the end, was made. It was used to pull the composite
bar for loading.

Fig 6.4: Fixture for cantilever beam bend test.

6.2.3 Cantilever bend test on MTS-810 Machine:

Figure 6.5 and 6.6 show the test setup and the mounting of fixture, loading arm and composite bar on MTS 810 machine. Initially the cantilever beam bend test was done on the composite bar at room temperature. Once the test setup was complete, the composite bar was loaded by the vertical movement of MTS head. The loading arm with a ring at one end pulls the composite while the other end is held between jaws of the sliding head. The load was increased in steps of Newton and the strain was measured from the signal-conditioning amplifier as voltage. Voltage readings for both tension and compression sides of the strain gages were taken simultaneously. For the bend test with the Liquid Nitrogen, the fixture walls were covered with Styrofoam (not shown in the figure) for insulation. Liquid Nitrogen was poured into the slot till the composite got fully immersed in it. When the strain gage output stabilized, the signal conditioning amplifier out was zeroed and the composite was loaded and the strain data was collected from both the tension and compression sides of the strain gages.

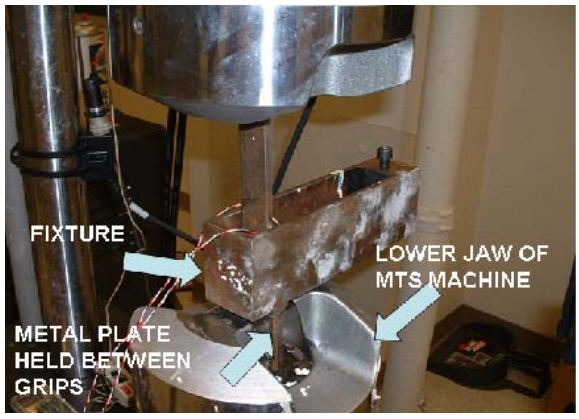

Fig: 6.5 Test setup on MTS machine.

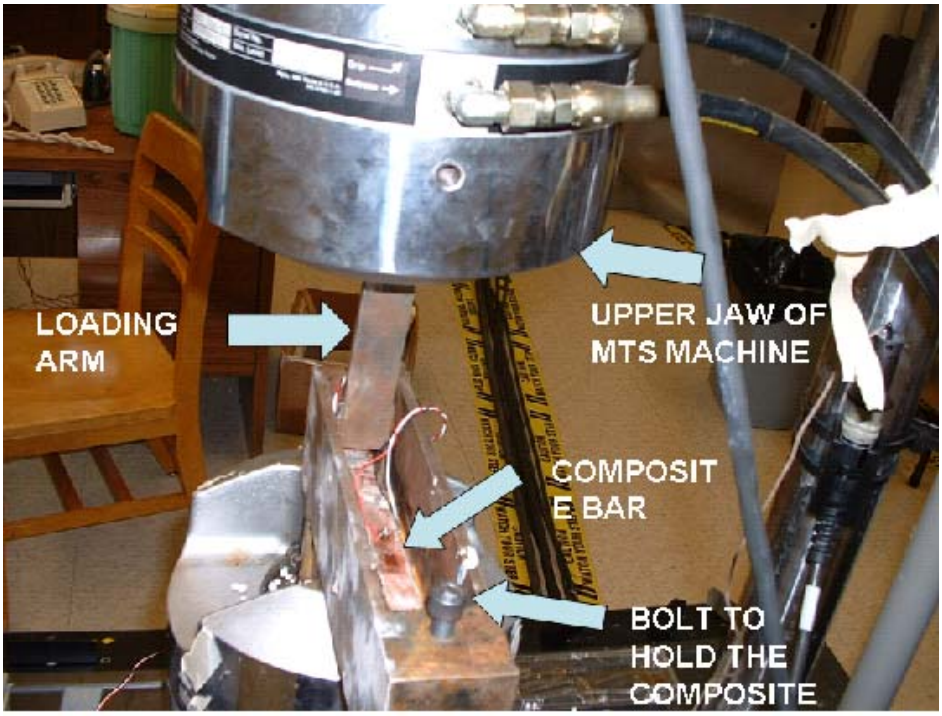

Fig 6.6: Mounting position of the fixture, loading arm and composite bar on MTS 810 machine

6.3 RESULTS:

Tables A.1 to A.4 in appendix show the strain data for the loading at room temperature and at liquid nitrogen temperature. The voltage data obtained from the signal conditioning amplifier was converted to strain data using an appropriate conversion. The load vs. the strain data was plotted for the tension and compression gages. Figure 6.7 shows the load vs. strain plots for the tension test data of composite bar at room temperature and at liquid nitrogen temperature. Figure 6.8 show the load vs. strain plots for the compression test data of composite bar at room temperature and liquid nitrogen temperature.

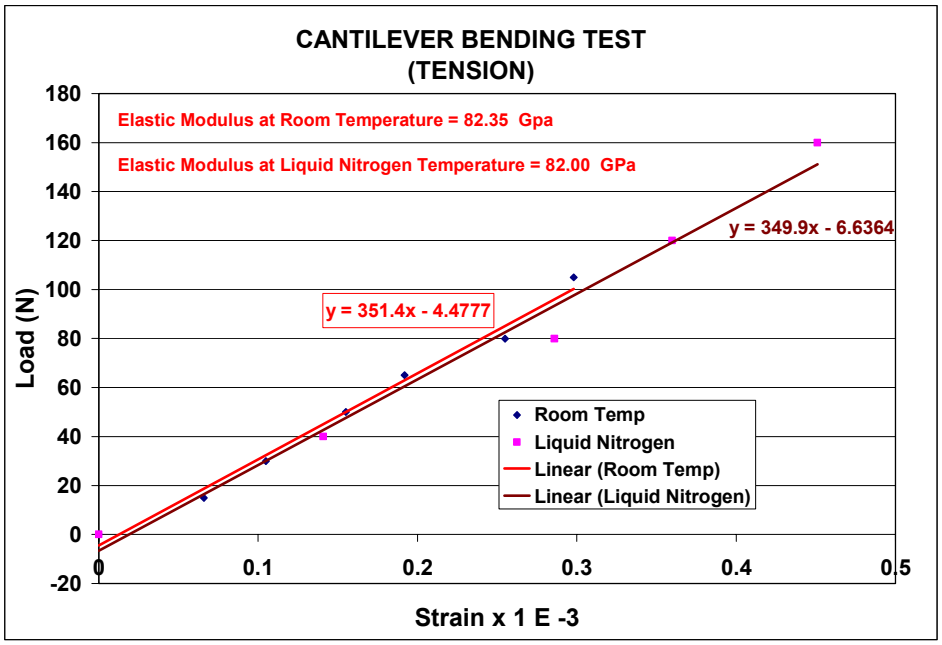

Fig 6.7: Load vs. Strain data for the composite bar in tension at room temperature and at Liquid Nitrogen Temperature.

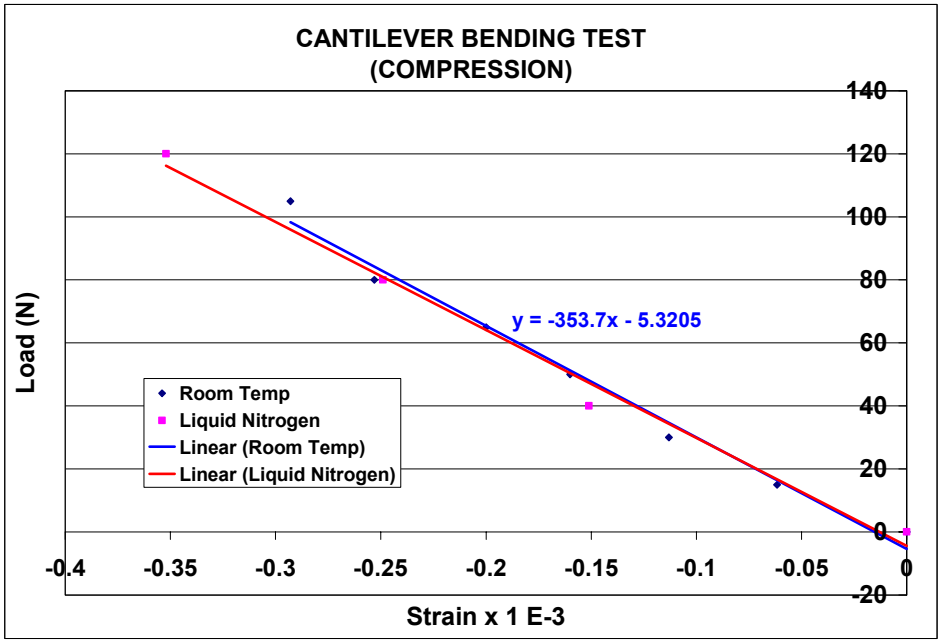

Fig 6.8: Load vs. Strain data for the composite bar in compression at room temperature and at Liquid Nitrogen Temperature.

Slope values from these plots were used to calculate the young's modulus of composite bar. Modulus of the composite was found using the formulae for cantilever beam theory. Table 6.1 shows the values of modulus for both the tests.

From the values shown in Table 6.1, we can see there isn't any significant change in the modulus of the composite at liquid nitrogen temperatures in comparison to the modulus value at room temperature.

Table 6.1 Elastic modulus value of CTD-101K-copper composite bar at room temperature and Liquid nitrogen temperature

	Cantilever in Tension Modulus (GPa)	Cantilever in Compression Modulus (GPa)
At room temperature	82.35	82.89
At Liquid Nitrogen temperature	82.00	80.34

7. CONCLUSIONS

The cure behavior of CTD-404 and CTD-101K was studied. Both polymers induced low cure stresses and high cool down stresses. CTD-404 with higher cross-link density induced larger stresses when compared to CTD-101K.

Also, a procedure for measuring the polymer modulus development during its cure has been developed. In this procedure, the cure-induced fiber load for a cure cycle was obtained from Cure Induced Stress Test (CIST). The polymer volume change for the same cycle was obtained from volumetric dilatometer. The modulus development was characterized from the difference in displacements of the polymer obtained from polymer volume and fiber load data. The modulus curves were scaled by using the experimental values from three-point bend tests available in literature for each cure cycle. The experimental values for partially cured samples were used to calibrate the modulus curve. A general agreement was found between the experimental modulus values and modulus curves. Since volumetric dilatometer was unavailable, the method was developed using the data for 3501-6.

The Young's Modulus of CTD-101K-copper composite in liquid nitrogen was determined. No significant change in the modulus value was observed when compared to the room temperature value.

8. PROPOSED FUTURE WORK

- The effect of relaxation of cure and cool down stresses induced on the modular coils by CTD-101K and CTD-404 has to be studied. The effect of relaxation on the modular coil geometry has to be verified.

- The method developed for the characterization of elastic modulus development has to be applied to CTD-404 and CTD-101K. The in cure volume change data for both the resins has to be obtained. Experimental modulus values of partially and completely cure samples of CTD-404 and CTD-101K have to be found.

REFERENCES

1. M. M. Schwartz, Composite Materials, Volume I: Properties, Nondestructive Testing and Repair, Prentice Hall PTR, 1996.

2. J.F.Lyon and the QPS team, "QPS, A Low Aspect Ratio Quasi-Poloidal Concept Exploration Experiment ", http://qps.fed.ornl.gov/pvr/pdf/qpsentire.pdf , April 2001.

3. Nelson, B., E., et. al, 'Design of the Quasi-Poloidal Stellarator Experiment', the 13th International Stellarator workshop, February 25—March 1 2002, paper no. PIIB.1.

4. S. Y. Lee and G. S. Springer, Journal of Composite Materials, 22, 15 (1988).

5. M. S. Madhukar, M. S. Genidy, and J. D. Russell, Journal of Reinforced Plastics and Composites, 18, 1304 (1999).

6. M. S. Madhukar, M.S. Genidy, and J. D. Russell, Journal of Composite Materials, 34, 1882 (2000).

7. M. S. Madhukar, M.S. Genidy, and J. D. Russell, Journal of Composite Materials, 34, 1905 (2000).

8. P.A. Fomitchov, Journal of Composite Materials, 36, 1889 (2002)

9. Degamber and Fernando, Plastics, Rubber and Composites, 32, 327 (2003)

10. M. Skrifvars et.al, Journal of Applied Polymer Science, 93, 1285 (2004)

11. K. Urabe, T. Okabe, H. Tsuda, Composites Science and Technology, 62, 791 (2001)

12. N. G. Pantelelis, A. Karamitsos, ANTEC 2003 Conference Proceedings, 3280(2003)

13. M.T. DeMeuse, J. K. Gillham, F. Parodi, Journal of Applied Polymer Science, 64, 15 (1997).

14. H.B. Wang, Yu-Geng Yang, Hui-Hong Yu, and Wei-Ming Sun, Polymer Engineering and Science, 35, 1895 (1995)

15. D.C. Blest et al, Composites: Part A, 30, 1289(1999)

16. A.A. Skordos, K. Partridge, Polymer Engineering and Science, 41, 793 (2001)

17. J.-L. Bailleul et.al, Composites: Part A, 34, 695 (2003)

18. Qi Zhu et.al, Journal of Composite Materials, 35, 2171 (2001)

19. S. R. White, H. T. Hahn, Journal of Composite Materials, 26, 2402 (1992)

20. S. R. White, H. T. Hahn, Journal of Composite Materials, 26, 2423 (1992)

21. A. K. Gopal et.al, Composite Structures, 48, 99 (2000)

22. D. J. O'Brien, P. T. Mather, and S. R. White, Journal of Composite Materials, 35, (10), 883 (2001).

23. S.L. Simon, G.B. McKenna, and O. Sindt, Journal of Applied Polymer Science, 76, (4), 495 (2000).

24. N. Meredith, Dental Materials, 15, 98–104 (1999)

25. Jakob Lange, Polymer Engineering and Science, 39, 1651 (1999)

26. Yongsong Eom, et.al, Polymer Engineering and Science, 40, 1281 (2000).

27. M. S. Madhukar, et.al, Society of Manufacturing Engineers, TP03PUB335 (2003).

28. M. S. Genidy, On the Reduction of Cure-Induced Stresses in Thermoset Polymer Composites, Ph.D. Dissertation, University of Tennessee, Knoxville, 1999.

29. R. L. Karkkainen, Empirical Modeling of In-Cure Volume Changes and Elasticity Development of Thermoset Polymers, M.S. Thesis, University of Tennessee, Knoxville, 2000.

30. H. Franks, Reduction of Cure-Induced Stresses in Thermoset Polymer Composites via Chemical and Thermal Methods, M.S. Thesis, University of Tennessee, Knoxville, 2003.

31. J.D. Russell, Analysis of Visco-elastic Properties of High –temperature Polymer using a Thermodynamic Equation of state, M.S. thesis, University of Dayton, 1991.

APPENDIX

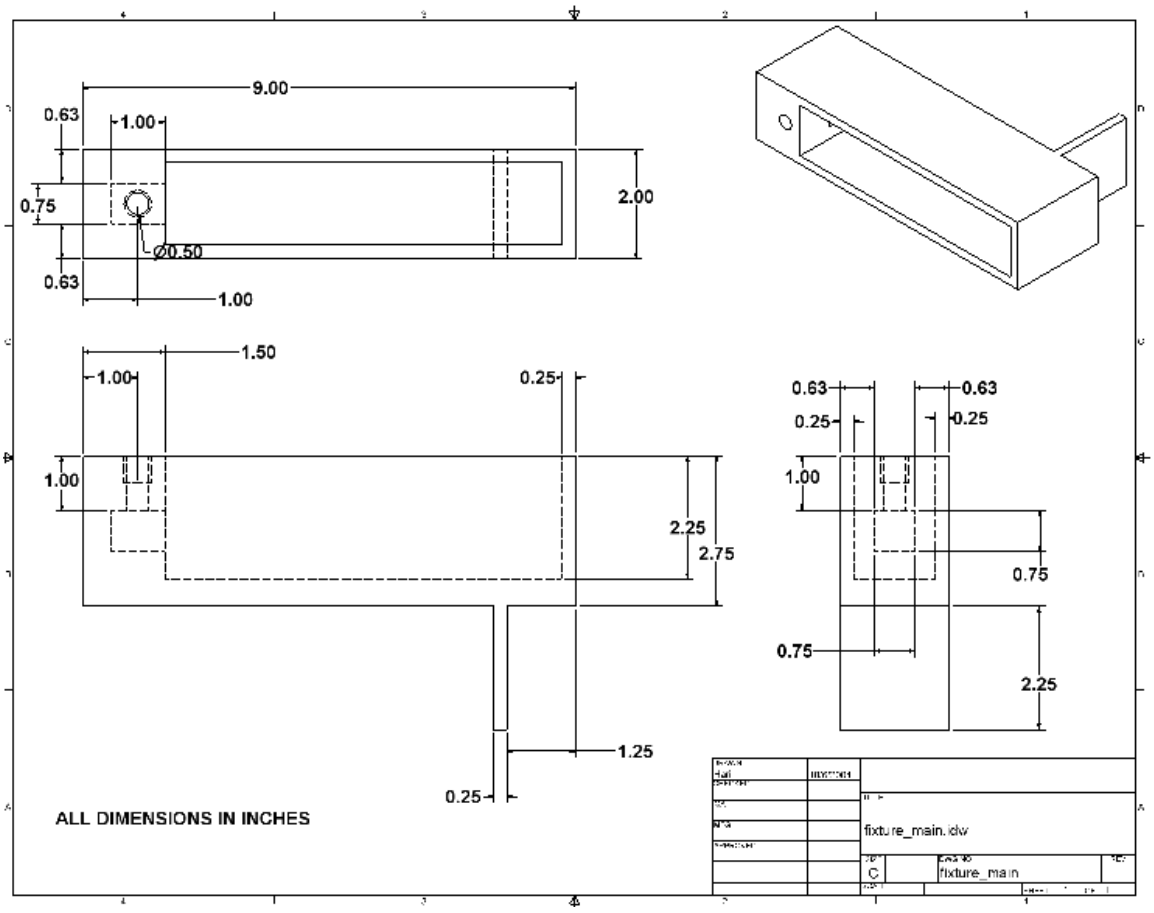

Fig A.1 Engineering drawing of the Fixture

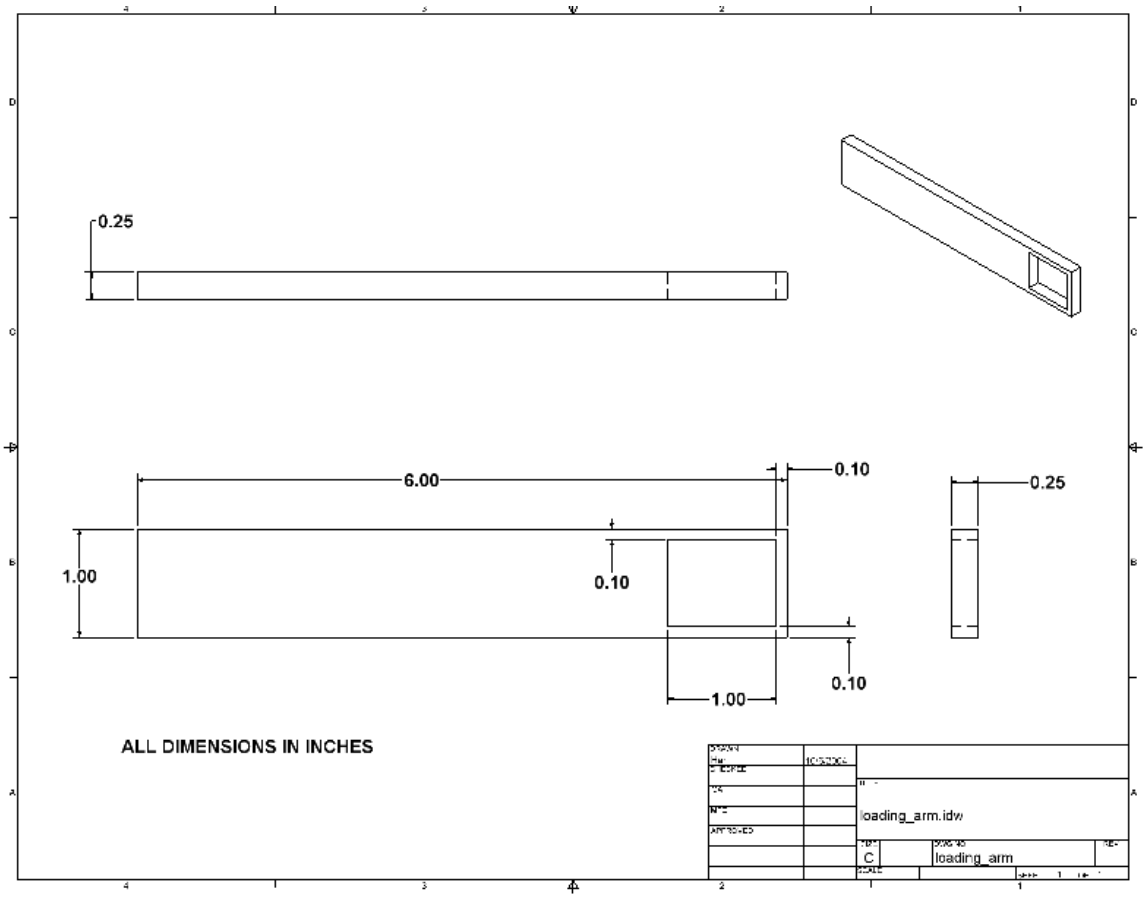

Fig A.2: Engineering drawing of the loading arm

Table A.1 Bend test data (Compression) at room temperature

Load (N)	Strain x 1E -6
0	0
15	-61.7
30	-113
50	-160
65	-200
80	-253
105	-293

Table A.2 Bend test data (Tension) at room temperature

Load (N)	Strain x 1 E -6
0	0
15	66
30	105
50	155
65	192
80	255
105	298

Table A.3 Bend test data (Compression) at Liquid Nitrogen temperature

Load (N)	Strain x 1 E-3
0	0
40	-0.151
80	-0.249
120	-0.352

Table A.4 Bend test data (Tension) at Liquid Nitrogen temperature

Load (N)	Strain x 1E-3
0	0
40	0.141
80	0.286
120	0.36
160	0.451

VITA

Hariharanath Kavuri was born on January 19th, 1981 in Machilipatnam, a small town in the state of Andhra Pradesh, India. He pursued his Bachelor's in Mechanical, Production and Industrial Engineering from Sagi Ramakrishnam Raju Engineering College in Bhimavaram, a privately owned college affiliated to Andhra University, Vizag, India. He was ranked 2nd among the students graduated in summer 2002, from Andhra University and affiliated colleges. Later he moved to The University of Tennessee, Knoxville in spring 2003 to pursue Master of Science in Mechanical Engineering. While pursuing his Master's program, he worked as a Graduate Research Assistant for Dr. Madhu S.Madhukar and was associated with Quasi Poloidal Nuclear Fusion Reactor Project of the Oak Ridge National Labs. As a Research Assistant, he worked on processing optimization and characterization of polymer composite materials. He will be graduating in December 2004 and will be seeking a professional position as an Engineer.